Self-Organized Criticality and the Development of EEG Phase Reset

Robert Wayne Thatcher,[1,2]* Duane Michael North,[2] and Carl John Biver[2]

[1]*Department of Neurology, University of South Florida College of Medicine, Tampa, Florida*
[2]*EEG and NeuroImaging Laboratory, Applied Neuroscience, Inc., St. Petersburg, Florida*

Abstract: *Objectives:* The purpose of this study was to explore human development of self-organized criticality as measured by EEG phase reset from infancy to 16 years of age. *Methods:* The electroencephalogram (EEG) was recorded from 19 scalp locations from 458 subjects ranging in age from 2 months to 16.67 years. Complex demodulation was used to compute instantaneous phase differences between pairs of electrodes and the 1st and 2nd derivatives were used to detect the sudden onset and offset times of a phase shift followed by an extended period of phase locking. Mean phase shift duration and phase locking intervals were computed for two symmetrical electrode arrays in the posterior-to-anterior locations and the anterior-to-posterior directions in the α frequency band (8–13 Hz). *Results:* Log–log spectral plots demonstrated $1/f^{\alpha}$ distributions ($\alpha \approx 1$) with longer slopes during periods of phase shifting than during periods of phase locking. The mean duration of phase locking (150–450 msec) and phase shift (45–67 msec) generally increased as a function of age. The mean duration of phase shift declined over age in the local frontal regions but increased in distant electrode pairs. Oscillations and growth spurts from mean age 0.4–16 years were consistently present. *Conclusions:* The development of increased phase stability in local systems is paralleled by lengthened periods of unstable phase in distant connections. Development of the number and/or density of synaptic connections is a likely order parameter to explain oscillations and growth spurts in self-organized criticality during human brain maturation. *Hum Brain Mapp 30:553–574, 2009.* **© 2008 Wiley-Liss, Inc.**

Key words: development of EEG phase reset; phase locking; chaos; self-organizational criticality

INTRODUCTION

Understanding the mechanisms of neural synchronization and desynchronization is important in understanding human brain dynamics. Recent studies have shown that sudden transitions in the amplitude of the human electroencephalogram (EEG) are represented by power laws and scale invariance and long-range temporal correlations [Freeman, 2003; Linkenkaer-Hansen et al., 2001; Nikulin and Brismar, 2005; Parish et al., 2004]. These studies are important because long-range temporal correlations are a reliable method to transfer information in neuronal populations as well as providing a linkage to general laws of physics of complex systems [Bak et al., 1987, 1988; Beggs and Plenz, 2003; Chialvo and Bak, 1999; Rios and Zang, 1999]. The rapid creation and destruction of multistable spatial-temporal patterns have been evaluated in evoked, transient, and spontaneous EEG studies [Breakspear and Terry, 2002a,b; Le Van Quyen, 2003; Rudrauf et al., 2006]. The patterns of spontaneously occurring synchronous activity involve the creation of differentiated and coherent neural assemblies at local, regional, and large scales [Breakspear and Terry, 2002a,b; Freeman and Rogers, 2002; Rudrauf et al., 2006; Stam and de Bruin, 2004; Varela, 1995]. The dynamic balance between synchronization and desynchronization is considered essential for normal brain function and abnormal balance is often associated with

*Correspondence to: Robert W. Thatcher, Neuroimaging Laboratory, Applied Neuroscience, Inc., St. Petersburg, Florida 33722, USA. E-mail: rwthatcher@yahoo.com

Received for publication 19 June 2007; Revised 9 October 2007; Accepted 2 November 2007

DOI: 10.1002/hbm.20524

Published online 24 January 2008 in Wiley InterScience (www.interscience.wiley.com).

pathological conditions such as epilepsy [Chevez et al., 2003; LeVan Quyen et al., 2001b; Lopes Da Silva and Pijn, 1995; Netoff and Schiff, 2002], schizophrenia [Lere et al., 2002] and dementia [Stam et al., 2002].

Synchronization is commonly defined as an "adjustment of rhythms of oscillating objects due to their weak interaction" and nearly always involves a period of stable phase relations or phase locking [Pikovsky et al., 2003]. Desynchronization is the opposite of synchronization and is defined as a shift in the phase difference of synchronized oscillators and elimination of phase locking. Notice that both synchronization and desynchronization start with a phase shift or adjustment but differ in the absence or extent of phase locking. Phase locking is a tell-tale sign of synchronization and this is why Freeman and coworkers [Freeman, 2003; Freeman and Rogers, 2002] and Breakspear and Williams [2004] and others [Lachaux et al., 2000; LeVan Quyen et al., 2001b] use phase locking as a measure of EEG synchronization.

The study of rapid changes in phase difference followed by periods of phase locking is called "phase reset" (PR). PR occurs in coupled nonlinear oscillators when there is a sudden shift of the phase relationship of oscillators to a new value followed by a period of phase locking or phase stability also called phase synchronization [Pikovsky et al., 2003]. The term phase synchrony is synonymous with phase locking and is sometimes preferred in order to emphasize the statistical nature of phase stability [Rudrauf et al., 2006]. However, the term phase synchrony is often used in reference to EEG coherence whereas phase locking is more specific to PR. Whether one refers to phase locking or phase synchrony what is important in the measurement of PR is that there is a prolonged period of phase stability following a phase shift. This is important because random phase shifts without stability exhibit "white noise" distributions [Pikovsky et al., 2003; Tass, 2007]. PR is also important because it results in increased EEG amplitudes because of increased phase locking of synaptic generators [Cooper et al., 1965; Lopes Da Silva, 1995; Nunez, 1995]. The integrated rapid sequencing of phase shifts followed by phase locking (i.e., the two fundamental components of PR) have been correlated to the α frequency band during cognitive tasks [Jensen and Lisman, 1998; Kahana, 2006; Kirschfeld, 2005; Tesche and Karhu, 2000], working memory [Damasio, 1989; John, 1968; Rizzuto et al., 2003; Tallon-Baudry et al., 2001], sensory-motor interactions [Roelfsema et al., 1997; Vaadia et al., 1995], hippocampal long-term potentiation [McCartney et al., 2004], and consciousness [Cosmelli et al., 2004; John, 2002, 2005; Varela et al., 2001]. The present study builds on these previous studies by parametrically analyzing the maturation of the two fundamental components of PR: (1) phase shift followed by, (2) phase stability in a large population of subjects from infancy to adolescence.

There are two general and equivalent methods for studying PR: (1) narrow band decomposition and, (2) broad band decomposition [Bruns, 2004; Le Van Quyen et al., 2001a; Rudrauf et al., 2006]. Both methods use analytic transforms such as the Fourier transform, Wavelet transform, and Hilbert transform. Which method is used depends on the frequency resolution desired and the nature of the transient signals that are to be detected [Freeman and Rogers, 2002; Freeman et al., 2003, 2006; Lachaux et al., 2000; Le Van Quyen et al., 2001a; Rudrauf et al., 2006; Tass, 2007]. In the present article, we used complex demodulation as an analytic signal processing method similar to Lachaux et al. [2000] and Breakspear and Williams [2004] which is mathematically the same as the Hilbert transform [Oppenheim and Schafer, 1975; Pikovsky et al., 2003]. All methods measure the phase difference of pairs of signals evaluated over successive intervals of time where phase stability is when the first derivative approximates zero or $d\varphi_{i,j}/dt \approx 0$. In general, the magnitude of phase shift is defined as the difference between the prephase shift value minus the postphase shift value and if a sudden and significant phase difference occurs followed by an extended period of phase stability then the point in time when the phase shift started is the time when the first derivative exceeded some threshold value [Breakspear and Williams, 2004; Le Van Quyen et al., 2001a; Rudrauf et al., 2006; Tass, 2007; Tass et al., 1998]. This point in time marks the onset of PR. EEG phase shift offset is defined in a reverse manner and the onset and offset times define the phase shift duration. The phase shift duration is typically in the range of 20–80 msec [Buzaski, 2006; Freeman, 2003; Freeman and Rogers, 2002]. Phase locking or phase stability that follows a phase shift is often 200–600 msec in duration in single cell analyses [Gray et al., 1989] and 100 msec to 1 second in surface recordings [Breakspear and Williams, 2004; Freeman and Baird, 1987; Freeman and Rogers, 2002; Freeman et al., 2006].

Recently, Linkenkaer-Hansen et al., [2001] Stam and de Bruin, [2004] Breakspear and Williams, [2004] Freeman et al. [2003, 2006], and Buzaski [2006] have shown that the EEG spectrum is best fit by a power function with a $1/f^{\alpha}$ distribution. The "one over f" distribution is shared by a very wide range of observations in the universe and was one of the intriguing mysteries in physics until Bak et al. [1987] created a mathematical and computer model of the process of $1/f$. Bak et al. [1987] referred to their model as "self-organized criticality" (SOC) because of their discovery of the spontaneous emergence of minimal stability with spatial scaling that leads to a $1/f$ power law for temporal fluctuations. Many studies have subsequently replicated and extended the mathematics and physics of SOC models [Bak, 1996]. An invariant feature of SOC is the presence of "activation–deactivation" processes and dissipation of energy which are fundamental to the $1/f$ distribution [Davidson and Schuster, 2000; Riuos and Zang, 1999]. The interplay of the dissipation and supply of energy from a source determines the amplitude and phase of all self-sustained nonlinear oscillators and activation–deactivation and dissipation are fundamental characteristics of neurons as well as most biological oscillators [Winfree, 1980; Pikovsky et al., 2003].The link of SOC models to EEG requires a minimum of three factors: (1) measurement of an activation–

deactivation process (e.g., rapid phase shift followed by stability), (2) an approximate $1/f$ distribution in a log–log plot and, (3) spatial scaling and temporal fluctuations where there are long-range temporal correlations [Bak, 1996; Bak et al., 1987, 1988; Davidson and Schuster, 2000]. The analyses of Freeman et al. [2003, 2006] and Breakspear and Williams [2004] demonstrated that the fine temporal structure of the EEG is characterized by $1/f$ distributions with periods of "unstable" phase dynamics followed by periods of "phase stability." These studies and others [Breakspear and Terry, 2002a,b] indicate that the human EEG fundamentally exhibits characteristics of "self-organizational criticality," where sudden phase shifts are "unstable phase dynamics" and phase locking or "phase synchrony" is "phase stability." Furthermore, these studies demonstrated that the terms "PR" and "SOC" when coupled with the $1/f$ distribution and activation–deactivation of self-sustaining nonlinear oscillators are synonymous terms in complex systems [Bak, 1996; Bak et al., 1987, 1988; Rios and Zang, 1999].

Currently, there are no studies of the early childhood development of EEG PR. Nikulin and Brismar [2005] studied EEG age dependence of $1/f^{\alpha}$ distributions in 96 adult subjects. Interesting age and gender correlations were presented, however, phase shift duration and phase locking were not separately analyzed. Developmental changes in the number of PRs per second and the duration of phase shifts and the length of phase locking are currently unknown and such information may be important in understanding the development of human neural dynamics. Therefore, the purpose of the present study is to investigate the development of human EEG PR from infancy to 16 years of age. The null hypotheses to be tested are: (1) there are no $1/f$ distributions of EEG phase reset, (2) there are no left and right hemispheric differences in the development of PR; (3) there are no differences in PR as a function of anterior-to-posterior versus posterior-to-anterior direction, (4) there are no differences in PR as a function of inter-electrode distance, (5) there are no changes in PR as a function of age.

METHODS

Subjects

A total of 458 subjects ranging in age from 2 months to 16.67 years (males = 257) were included in this study. The subjects in the study were recruited using newspaper advertisements in rural and urban Maryland [Thatcher et al., 1987, 2003, 2007]. The inclusion/exclusion criteria were no history of neurological disorders such as epilepsy, head injuries and reported normal development and successful school performance. None of the subjects had taken medication of any kind at least 24 h before testing. All of the subjects were within the normal range of intelligence as measured by the WISC-R and were performing at grade level in reading, spelling and arithmetic as measured by the WRAT and none were classified as learning disabled nor were any of the school aged children in special education classes. All subjects $\geq$2 years of age were given an eight-item "laterality" test consisting of three tasks to determine eye dominance, two tasks to determine foot dominance, and three tasks to determine hand dominance. Scores ranged from -8 (representing strong sinistral preference or left handedness), to $+8$ (representing strong dextral preference or right handedness). Dextral dominant children were defined as having a laterality score of $\geq$2 and sinistral dominant children were defined as having a laterality score of ≤ -2. Only 9% of the subjects had laterality scores ≤ -2 and 87% of the subjects had laterality scores $\geq$2 and thus the majority of subjects were right side dominant.

EEG Recording

Power spectral analyses were performed on 58 sec to 2 min 17 sec segments of EEG recorded during the resting eyes closed condition. The EEG was recorded from 19 scalp locations based on the International 10/20 system of electrode placement, using linked ears as a reference. The average reference and a Laplacian reference were not used because these reference methods involve mixing the amplitude and phase from different scalp locations resulting in phase and coherence distortions as shown by Rappelsberger [1989], Kamiński et al. [1997], and Essl and Rappelsberger [1998]. Eye movement electrodes were applied to monitor artifact and all EEG records were visually inspected and manually edited to remove any visible artifact. Each EEG record was plotted and visually examined and split-half reliability and test re-test reliability measures of the artifacted data were computed using the Neuroguide software program (NeuroGuide, v2.3.8). Split-half reliability tests were conducted on the edited EEG segments and only records with >90% reliability were entered into the spectral analyses. The amplifier bandwidths were nominally 1.0–30 Hz, the outputs being 3 db down at these frequencies. The EEG was digitized at 100 Hz and upsampled to 128 Hz and then spectral analyzed using complex demodulation [Granger and Hatanaka, 1964; Otnes and Enochson, 1978] (see section Complex Demodulation and Joint-Time-Frequency-Analysis).

EEG phase differences and PR metrics were computed in the α frequency band (8.0–13.0 Hz) for anterior-to-posterior electrodes Fp1/2-F3/4; Fp1/2-C3/4; Fp1/2-P3/4, and Fp1/2-O1/2 and for posterior-to-anterior electrodes O1/2-P3/4; O1/2-C3/4; O1/2-F3/4 and O1/2-Fp1/2. This recording arrangement provides a stable matrix and test of spatial homogeneity by using five equally spaced electrodes per hemisphere with increasing distance between electrodes in the anterior-to-posterior and posterior-to-anterior directions. According to volume conduction there is a homogeneous decline of voltage as a function of distance from any source at near zero phase delay. The five equally spaced electrode locations is a direct test of volume conduction versus cortical connectivity [Thatcher et al., 1986, 1998; 2007]. Factors used in the multivariate analysis of

variance were: (1) Hemisphere, (2) Direction, (3) Inter-electrode distance, and (4) Age. The analyses of different frequency bands demonstrated that the α frequency band exhibits the strongest developmental trends and, therefore, this study will focus exclusively on the 8–13 Hz α frequency band [Niedermeyer and Lopes da Silva, 2005].

Complex Demodulation and Joint-Time-Frequency-Analysis

Complex demodulation was used in a joint-time-frequency-analysis (JTFA) to compute instantaneous coherence and phase-differences [Bloomfield, 2000; Granger and Hatanaka, 1964; Otnes and Enochson, 1978]. This method is an analytic linear shift-invariant transform that first multiplies a time series by the complex function of a sine and cosine at a specific center frequency (Center frequency = 10.0 Hz) followed by a low pass filter (6th order low-pass Butterworth, bandwidth = 2.0 Hz) which removes all but very low frequencies (shifts frequency to 0) and transforms the time series into instantaneous amplitude and phase and an "instantaneous" spectrum [Bloomfield, 2000]. We place quotations around the term "instantaneous" to emphasize that, as with the Hilbert transform, there is always a trade-off between time resolution and frequency resolution. The broader the band width the higher the time resolution but the lower the frequency resolution and vice versa. Mathematically, complex demodulation is defined as an analytic transform (Z transform) that involves the multiplication of a discrete time series $\{x_t, t = 1, \ldots, n\}$ by $\sin \omega_0 t$ and $\cos \omega_0 t$ giving

$$x'_t = x_t \sin \omega_0 t \tag{1}$$

and

$$x''_t = x_t \cos \omega_0 t \tag{2}$$

and then apply a low pass filter F to produce the instantaneous time series, Z'_t and Z''_t where the sine and cosine time series are defined as:

$$Z'_t = F(x_t \sin \omega_0 t) \tag{3}$$

$$Z''_t = F(x_t \cos \omega_0 t) \tag{4}$$

and

$$2[(Z'_t)^2 + (Z''_t)^2]^{1/2} \tag{5}$$

is an estimate of the instantaneous amplitude of the frequency ω_0 at time t and

$$\tan^{-1} \frac{Z'_t}{Z''_t} \tag{6}$$

is an estimate of the instantaneous phase at time t. At this step the complex demodulation transform is the same as the Hilbert transform [Oppenheim and Schafer, 1975; Pikovsky et al., 2003, p. 362].

The instantaneous cross-spectrum is computed when there are two time series $\{y_t, t = 1,\ldots, n\}$ and $\{y'_t, t = 1, \ldots, n\}$ and if $\boldsymbol{F}$ [ ] is a filter passing only frequencies near zero, then, as above $R_t^2 = F[y_t \sin \omega_0 t]^2 + F[y_t \cos \omega_0 t]^2 = |F[y_t e^{i\omega_0 t}]^2|$ is the estimate of the amplitude of frequency ω_0 at time t and $\varphi_t = \tan^{-1}\left(\frac{F[y_t \sin \omega_0 t]}{F[y_t \cos \omega_0 t])}\right)$ is an estimate of the phase of frequency ω_0 at time t and therefore,

$$F[y_t e^{i\omega_0 t}] = R_t e^{i\varphi_t}, \tag{7}$$

and likewise

$$F[y'_t e^{i\omega_0 t}] = R'_t e^{i\varphi_t} \tag{8}$$

The instantaneous cross-spectrum is

$$V_t = F[y_t e^{i\omega_0 t}] F[y'_t e^{-i\omega_0 t}] = R_t R'_t e^{i[\varphi_t - \varphi'_t]} \tag{9}$$

and the instantaneous coherence is

$$\frac{|V_t|}{R_t^2 R_t'^2} \equiv 1 \tag{10}$$

The instantaneous phase-difference is $\varphi_t - \varphi'_t$. That is, the instantaneous phase difference is computed by estimating the instantaneous phase for each time series separately and then taking the difference. Instantaneous phase difference is also the arctangent of the imaginary part of V_t divided by the real part (or the instantaneous quadspectrum divided by the instantaneous cospectrum) at each time point.

Phase Straightening

We used the phase "straightening" method of Otnes and Enochson [1978] to remove the phase angle discontinuity, i.e., where 0 and 360 are at opposite ends while in the circular distribution $0^\circ = 360^\circ$. The Otnes and Enochson [1978] procedure involves identifying the points in time when phase jumps from $+180^\circ$ to -180° and then adding or subtracting 360° depending on the direction of sign change. For example, $\Delta\theta = (180 - \varepsilon)^\circ + (180 - \varepsilon)^\circ = 360^\circ - 2\varepsilon$ which is the same as 2ε since $-(180 - \varepsilon)^\circ = 180 + \varepsilon$. This procedure results in phase being a smooth function of time and removes the discontinuities due to the arctangent function. We found that absolute phase differences without phase straightening gave similar results to the straightened phase differences. This is because the vast majority of EEG phase relationships are less than $\pm 180^\circ$. However, phase straightening is important when computing the first and second derivatives of the time series of phase differences because the discontinuity between -180° to $+180^\circ$ can produce artifacts. Accordingly, all of the derivatives and

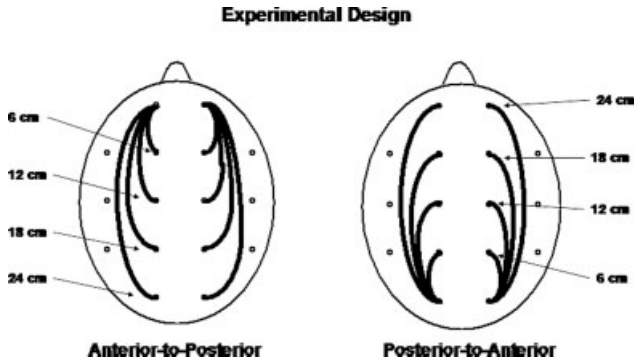

Figure 1.
Experimental design. Left head diagram shows the location of electrodes for the computation of coherence and phase differences in the anterior-to-posterior direction. Right head diagram shows the location of electrodes in the posterior-to-anterior direction. Local distances (6 cm) are in adjacent electrode combinations (O1/2-P3/4 and Fp1/2-F3/4). Longest distance (24 cm) electrode combinations are Fp1/2-O1/2.

PR measures in this article were computed after phase straightening.

Computation of the 1st and 2nd Derivatives of the Time Series of Phase Differences

The first derivative of the time series of phase-differences between all pair wise combinations of two channels was computed in order to detect advancements and reductions of phase-differences. The Savitzgy-Golay procedure was used to compute the first derivatives of the time series of instantaneous phase differences using a window length of 3 time points and the polynomial degree of 2 [Press et al., 1994; Savitzgy-Golay, 1964]. The units of the 1st derivative are in degrees/point which was normalized to degrees per centisecond (i.e., degrees/csec = degrees/100 msec). The second derivative was computed using a window length of 5 time points and a polynomial degree of 3 and the units are degrees per centiseconds squared (i.e., degrees/csec^2 = degrees/100 msec^2.)

Calculation of Phase Reset

The time series of 1st derivatives of the phase difference from any pair of electrodes was first rectified to the absolute value of the 1st derivative (see Fig. 2). The sign or direction of a phase shift is arbitrary since two oscillating events may "spontaneously" adjust phase with no starting point [Pikovsky et al., 2003; Tass, 2007]. The onset of a phase shift was defined as a significant absolute first derivative of the time series of phase differences between two channels, i.e., $d(\varphi_t - \varphi'_t)/dt > 0$, criterion bounds = 5°. Phase stability or phase locking is defined as that period of time after a phase shift where there is a stable near zero first derivative of the instantaneous phase differences or $d(\varphi_t - \varphi'_t)/dt \approx 0$. The criteria for a significant 1st derivative is important and in the present study a threshold criteria of 5° was selected because it was >3 standard deviations where the mean phase shift ranged from 25°/csec to 45°/csec. Changing the threshold to higher values was not significant, however, eliminating the threshold resulted in greater "noise" and therefore the criteria of 5° is an adequate criteria. As pointed out by Breakspear and Williams [2004] visual inspection of the data is the best method for selecting an arbitrary threshold value and the threshold value itself is less important than keeping the threshold constant for all subjects and all conditions. Figure 2 illustrates the concept of PR. Phase differences over time on the unit circle are measured by the length of the unit vector r. Coherence is a measure of phase consistency or phase clustering on the unit circle as measured by the length of the unit vector r. The illustration in Figure 2 shows that the resultant vector $r_1 = r_2$ and therefore coherence when averaged over time ≈ 1.0 even though there is a brief phase shift. As the number of phase shifts per unit time increases then coherence declines because coherence is directly related to the average amount of phase locking or phase synchrony [Bendat and Piersol, 1980].

Figure 3 shows the time markers and definitions used in this study. As mentioned earlier the peak of the absolute 1st derivative was used in the detection of the onset and offset of a phase shift and the second derivative was used to detect the inflection point which defines the full-width-half-maximum (FWHM) and phase shift duration. As seen in Figure 3, PR is composed of two events: (1) a phase shift of a finite duration (SD) and (2), followed by an extended period of phase locking as measured by the phase locking interval (LI) and PR = SD + SI. Phase Shift duration (SD) is the interval of time from the onset of phase shift to the termination of phase shift where the termination is defined by two conditions: (1) a peak in the 1st derivative (i.e., 1st derivative changes sign from positive to zero to negative) and, (2) a peak in the 2nd derivative or inflection on the declining side of the time series of first derivatives. The peak of the 2nd derivative marked the end of the phase shift period. Phase shift duration is the difference in time between phase shift onset and phase shift offset or $SD(t) = S(t)_{onset} - S(t)_{offset}$. Phase locking interval (LI) was defined as the interval of time between the end of a significant phase shift (i.e., peak of the 2nd derivative) and the beginning of a subsequent significant phase shift, i.e., marked by the peak of the 2nd derivative and the presence of a peak in the 1st derivative or $SI(t) = S(t)_{offset} - S(t)_{onset}$. See Figure 3 is a diagram of phase shift duration and phase locking intervals. In summary, two measures of phase dynamics were computed: (1) Phase shift duration (msec) (SD) and, (2) Phase locking interval (msec) (LI). Figure 3 illustrates the PR metrics and Figure 4 shows an example of the computation of PR metrics in a single subject.

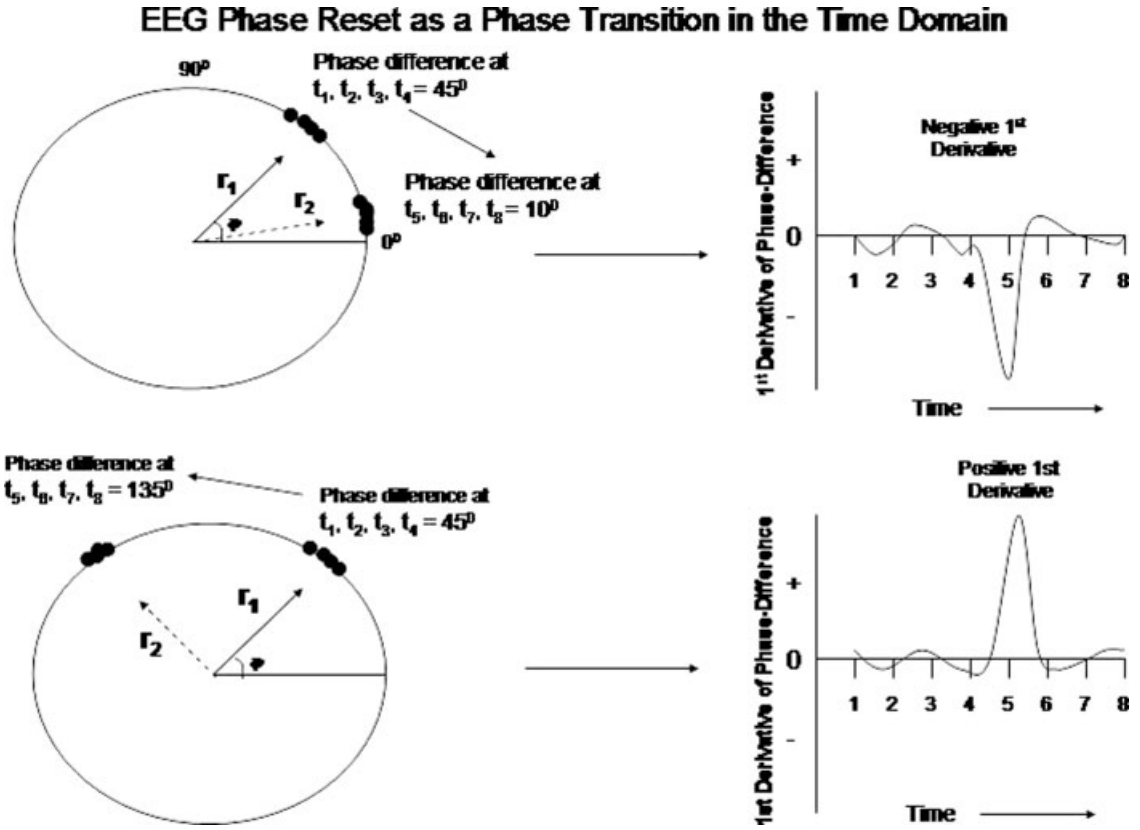

Figure 2.

Illustrations of phase reset. Left is the unit circle in which there is a clustering of phase angles and thus high coherence as measured by the length of the unit vector r. The top row is an example of phase reduction and the top right is a time series of the approximated 1st derivative of the instantaneous phase differences for the time series t_1, t_2, t_3, t_4 at mean phase angle = 45° and t_5,t_6,t_7, t_8 at mean phase angle = 10°. The vector r1 = 45° occurs first in time and the vector r2 = 10° and 135° (see bottom left) occurs later in time. Phase reset is defined by a sudden change in phase difference followed by a period of phase locking. The onset of Phase Reset is between time point 4 and 5 where the 1st derivative is a maximum. The 1st derivative near zero is when there is phase locking and little change in phase difference over time. The bottom row is an example of phase advancement and the bottom right is the 1st derivative time series. The sign or direction of phase reset is arbitrary since two oscillating events are being brought into phase locking and represent a stable state as measured by the 1st derivative independent of direction.

Sliding Averages

To increase temporal resolution 1 year sliding averages of EEG phase differences were computed. The procedure involved computing means and standard deviations for phase locking intervals and phase shift intervals over a 1-year period, e.g., birth to 1 year, then computing means and standard deviations from 0.25–1.25 years, then a mean and standard deviation for the ages from 0.5–1.5 years, etc. This resulted in a 75% overlap of subjects per mean with totally unique subjects on a 1-year interval. The sliding average procedure produced 64 equally spaced mean values with a 0.25 year resolution. Table I shows the age range per bin, the mean ages per bin and the number of subjects per age group from mean age of 0.4–16.2 years. Relative small *N*s were present from 0.4–1.4 years of age and larger sample sizes (max $N = 50$) were present beyond 1 year of age. In spite of the relatively small sample sizes at 0.4–1.4 years the mean values of phase shift and PR were well behaved and stable (see Figs. 7 and 8). The overall average number of subjects per age bin = 28.5.

Spectral Analyses of 1/*f* distribution

To evaluate possible $1/f$ spectral distributions the fast Fourier transform (FFT) of the time series of the 1st derivative of phase differences were computed for individual subjects using edited EEG data. The FFT epoch length was 2 sec and the sample rate was 128 Hz. Computations were first conducted on the entire edited EEG record (58 sec to 2 min 17 sec) and then separate selections of periods of

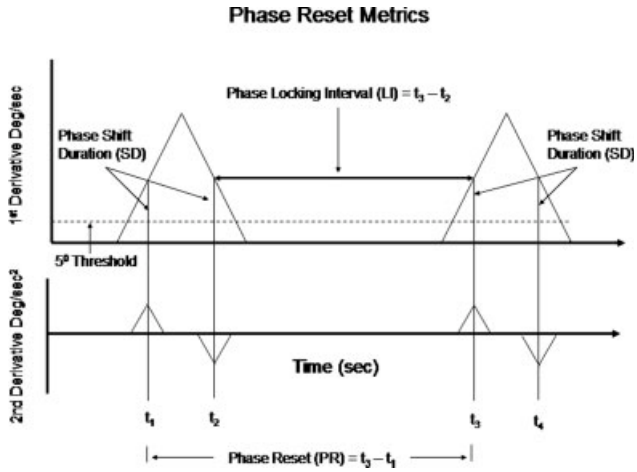

Figure 3.
Diagram of phase reset metrics. Phase shift (PS) onset was defined at the time point when a significant 1st derivative occurred ($\geq 5^{\circ}$/csec) followed by a peak in the 2nd derivative and a peak in the 1st derivative, phase shift duration (SD) was defined as the time from onset of the phase shift defined by the positive peak of the 2nd derivative to the offset of the phase shift defined by the negative peak of the 2nd derivative. The phase locking interval (LI) was defined as the interval of time between the onset of a phase shift and the onset of a subsequent phase shift. Phase reset (PR) is composed of two events: (1) a phase shift and (2) a period of locking following the phase shift where the 1st derivative $\approx$ 0 or PR = SD + LI.

phase shift and phase locking were subjected to separate FFT analyses in order to determine if the spectra were different between the phase locking versus the phase shift periods in the EEG record. Tests of the $1/f$ distribution involved plotting the $\log_{10}$ transforms of frequency and magnitude and then a linear regression was used to determine the slope (α coefficient) and intercept of the linear fit.

Spectral Analyses of Developmental Ultraslow Oscillations During the Lifespan

As explained previously, the sliding averages produced 64 equally spaced mean values of phase shift duration and phase locking intervals in each electrode pairing (at 3 month or 0.25 year resolution) from 0.4–16.2 years. This resulted in a developmental time series of equally spaced mean ages for phase shift duration and phase locking intervals which were then spectrally analyzed. The Fast Fourier Transform (FFT) was used to analyze the frequency spectrum of the developmental trajectories of phase shift and phase locking. Detrending was used prior to the FFT to remove the low frequency developmental trends in order to analyze the frequency and power of rhythmic changes during the developmental period. The number of time points = 64, and the epoch length or Lifespan = 16.2 years. This produced a frequency resolution of 6 months and a maximum frequency of 32 cycles per epoch. The units of frequency were cycles per lifespan (cpl) and wavelength (λ) = 16.2/cpl. The units of frequency are cpl. The magnitude of the spectrum plotted on the *y*-axis are milliseconds/cycle/lifespan or msec/cpl.

RESULTS

1/*f* Distributions

As discussed in the introduction, the human EEG is often characterized by $1/f$ distributions which are revealed by log–log plots of the power spectrum [Buzsaki, 2006; Freeman et al., 2003, 2006]. All of the subjects exhibited $1/f$ distributions of the 1st derivative of phase differences. Figure 5 shows examples of linear regression fits of the log–log plots of the power spectrum of the 1st derivative of phase differences in four subjects in the anterior-to-posterior direction. Very similar spectra were obtained independent of direction of hemisphere. Table II, shows the slope or α values, the intercept and the regression correlation coefficients which all yielded $1/f^{\alpha}$ spectral distributions with a range from -0.86 to -0.54 and the average $\alpha = -0.76$. To further investigate the nature of the $1/f$ distribution, subcomponent analyses were conducted by selecting the 1st derivative of phase difference during PR by separately selecting the phase shift periods and phase locking periods and then spectrally analyzing the two different data selections. Frequency and magnitude were $\log_{10}$ transformed and linear regression fits were conducted in order to determine the slopes of the spectra. The results of the subcomponent analyses are shown in Figure 6 and Table III. In all instances and in all subjects, the slope of the linear fit was >1.0 for phase locking and <1.0 for phase shift periods. The average slope or α coefficient was close to 1.0 with a mean = 1.0466. As seen in Table III, there were statistically significant differences in slope (i.e., α) between periods of phase shift versus periods of phase locking where the slope was always steeper for phase locking than phase shift. Although all of the regression fits were statistically significant, nonetheless, the linear fit for phase locking accounted for less variance than for phase shift duration which is likely due to the exponential shape of the phase locking spectral distribution.

Table III shows the alpha slope values and age regression correlations and *t*-tests between the spectral distributions for phase shift versus phase locking intervals for the four sample subjects in Figure 6. The α values for phase shift were statistically significantly smaller than the α values for phase locking and the average α value was close to 1.0 which indicates that decomposition of the log–log spectral distribution into subcomponents of phase shift versus phase locking is useful in order to reveal more of the underlying EEG dynamics.

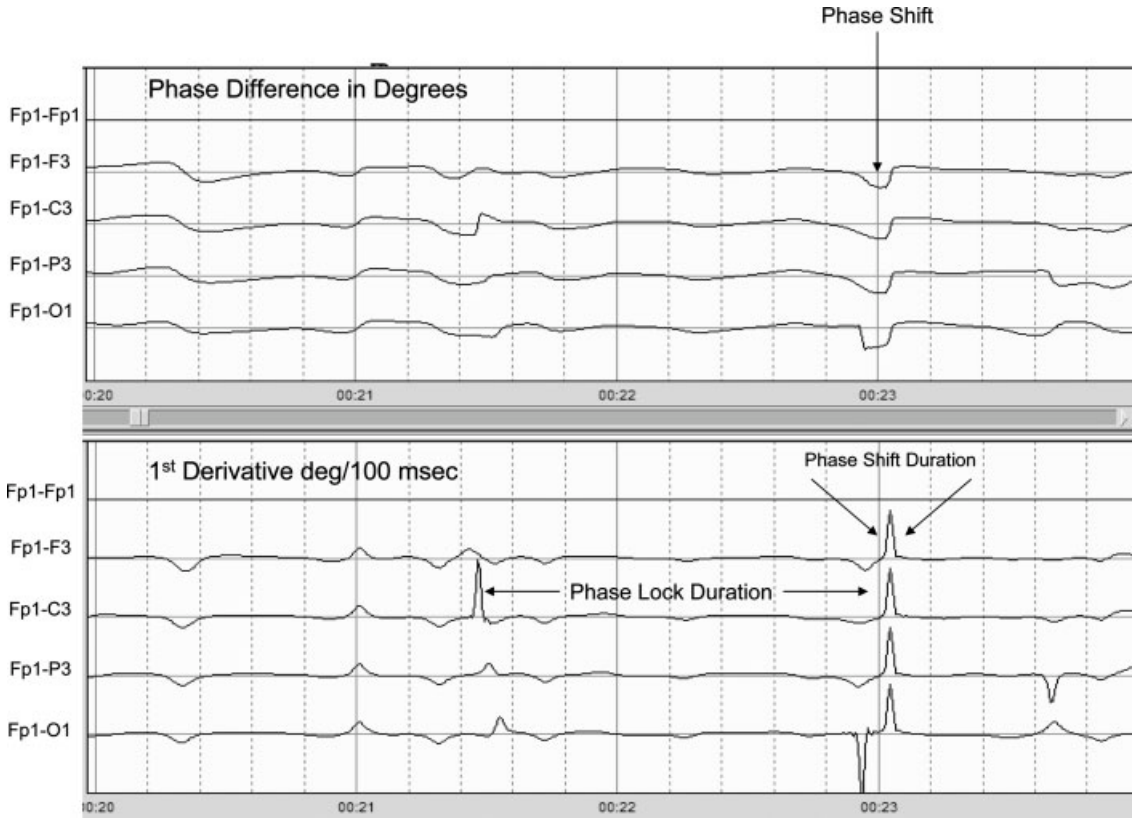

Figure 4.

Example from one subject. Top are the EEG phase differences between Fp1-F3, Fp1-C3, Fp1-P3 and Fp1-O1 in degrees. Bottom are the 1st derivatives of the phase differences in the top traces in degrees/centiseconds. A 1st derivative $\geq 5^{\circ}$/csec marked the onset of a phase shift and an interval of time following the phase shift where the 1st derivative ≈ 0 defined the phase locking interval as described in Figure 3.

Development of Phase Shift Duration

Figure 7 shows the mean duration of phase shift in the α frequency band from 0.4–16.2 years of age. The top row are mean phase shift duration values in the anterior-to-posterior direction (see Fig. 1) and the bottom row are the posterior-to-anterior electrode combinations. The left column is the mean phase shift durations for the left hemisphere and the right column are the right hemisphere values. It can be seen that there were oscillations and sudden changes in the mean duration of phase shift and there was a steady increase in the mean duration of phase shift as a function of age in the long inter-electrode distances (18 and 24 cm) and reduced phase shift duration in the short inter-electrode distance (6 cm) in anterior-posterior directions. In the posterior-anterior direction, an increase in phase shift duration was present as a function of age in all inter-electrode distances, although the long inter-electrode distances (18 and 24 cm) exhibited a more pronounced increase in phase duration with age than the short inter-electrode distances (6 cm).

Table IV shows the results of a linear fit of the mean duration of phase shift as a function of age for all electrode pairings. It can be seen in Table IV that there were statistically significant negative slopes in the short inter-electrode distance (6 cm) in the anterior-posterior direction and positive slopes in all other instances. Statistically, significant age regressions were present for all of the developmental trajectories.

Multivariate analyses of variance (MANOVA) were conducted with the factors being direction (anterior-to-posterior versus posterior-to-anterior), left hemisphere versus right hemisphere and distance (6, 12, 18, and 24 cm). No significant left versus right hemisphere affect was present ($F = 0.2345$, $P < 0.628$). However, there was a statistically significant direction affect ($F = 303.73$, $P < 0.0001$) with a statistically significant Bonferroni post hoc test ($P < 0.0001$). There was also a statically significant distance affect ($F = 350.21$, $P < 0.0001$) with statistically significant Bonferroni post hoc tests ($P >$,0001) for all inter-electrode distances except for 24–18 cm ($P < 0.68$).

TABLE I. Age ranges, mean ages, and the number of subjects per age bin using sliding average computation

Age bins	Mean age	*N*-size
0.00–.00	0.4	7
0.25–.25	0.7	5
0.50–.50	1.1	7
0.75–.75	1.4	9
1.00–2.00	1.6	11
1.25–2.25	1.8	14
1.50–2.50	2.0	14
1.75–2.75	2.2	11
2.00–3.00	2.6	14
2.25–3.25	2.8	13
2.50–3.50	3.0	13
2.75–3.75	3.2	14
3.00–4.00	3.5	13
3.25–4.25	3.9	15
3.50–4.50	4.0	15
3.75–4.75	4.2	17
4.00–5.00	4.4	16
4.25–5.25	4.9	19
4.50–5.50	5.0	23
4.75–5.75	5.3	28
5.00–6.00	5.5	34
5.25–6.25	5.8	36
5.50–6.50	6.0	35
5.75–6.75	6.2	34
6.00–7.00	6.5	38
6.25–7.25	6.8	33
6.50–7.50	7.0	40
6.75–7.75	7.3	44
7.00–8.00	7.5	47
7.25–8.25	7.7	48
7.50–8.50	8.0	45
7.75–8.75	8.2	40
8.00–9.00	8.4	32
8.25–9.25	8.7	28
8.50–9.50	9.0	26
8.75–9.75	9.3	29
9.00–10.00	9.6	38
9.25–10.25	9.8	45
9.50–10.50	10.0	46
9.75–10.75	10.2	45
10.00–11.00	10.4	40
10.25–11.25	10.8	40
10.50–11.50	11.0	43
10.75–11.75	11.3	47
11.00–12.00	11.5	50
11.25–12.25	11.7	42
11.50–12.50	11.9	40
11.75–12.75	12.3	39
12.00–13.00	12.5	39
12.25–13.25	12.7	41
12.50–13.50	13.0	41
12.75–13.75	13.3	38
13.00–14.00	13.5	41
13.25–14.25	13.7	38
13.50–14.50	13.9	36
13.75–14.75	14.2	30
14.00–15.00	14.4	24
14.25–15.25	14.7	23
14.50–15.50	14.9	20
14.75–15.75	15.3	17
15.00–16.00	15.5	16
15.25–16.25	15.7	12
15.50–16.50	15.8	11
15.75–16.75	16.2	12

Development of the Phase Locking Interval

Figure 8 shows the mean phase locking interval in the α frequency band from 0.4–16.2 years of age. The top row is mean phase locking interval values in the anterior-to-posterior direction (see Fig. 1) and the bottom row are the posterior-to-anterior electrode combinations. The left column is the mean phase locking intervals for the left hemisphere and the right column are the right hemisphere values. It can be seen that there were oscillations and sudden changes in the mean phase locking intervals and there was a steady increase in the mean phase locking interval as a function of age in the short inter-electrode distance (6 cm) with less increased phase locking intervals in the long inter-electrode distances. Sudden increases in the mean phase locking interval were present n all electrode combinations at ages 9 and 14 years, especially in the short inter-electrode distances (6 cm) and in the posterior-to-anterior direction.

Table V shows the results of a linear fit of the mean phase locking interval as a function of age for all electrode pairings. It can be seen in Table V that there were statistically significant positive slopes in all instances. The short inter-electrode distance (6 cm) exhibited a steeper developmental slope in the posterior-to-anterior direction than in the anterior-to-posterior direction.

Multivariate analyses of variance (MANOVA) were conducted with the factors being direction (anterior-to-posterior versus posterior-to-anterior), left hemisphere versus right hemisphere and distance (6, 12, 18, and 24 cm). No significant left versus right hemisphere affect was present ($F = 3.033$, $P < 0.082$). However, there was a statistically significant direction affect ($F = 82.02$, $P < 0.0001$) with a statistically significant Bonferroni post hoc test ($P < 0.0001$). There was also a statically significant distance affect ($F = 173.55$, $P < 0.0001$) with statistically significant Bonferroni post hoc tests ($P > 0.0001$) for all inter-electrode distances except for 24–12 cm ($P < 0.271$) and 24–18 cm ($P < 0.783$).

Relations Between Phase Reset and Coherence

Coherence is a measure of phase stability and one would expect a positive correlation between the duration of phase locking and coherence. We tested this hypothesis using a Pearson product correlation coefficient of the developmental time series of coherence and phase shift duration and phase locking interval in the short inter-electrode distances (6 cm). Table VI shows the average correlation of the short inter-electrode distance measures in which there was a negative correlation between coherence and phase shift duration (i.e., inverse relationship to "unstable phase dynamics") and a positive correlation between coherence and phase locking intervals (i.e., direct relationship to "Stability"). The hypothesis of a positive relationship between coherence and phase locking was confirmed. As expected there was an inverse relationship between phase shift

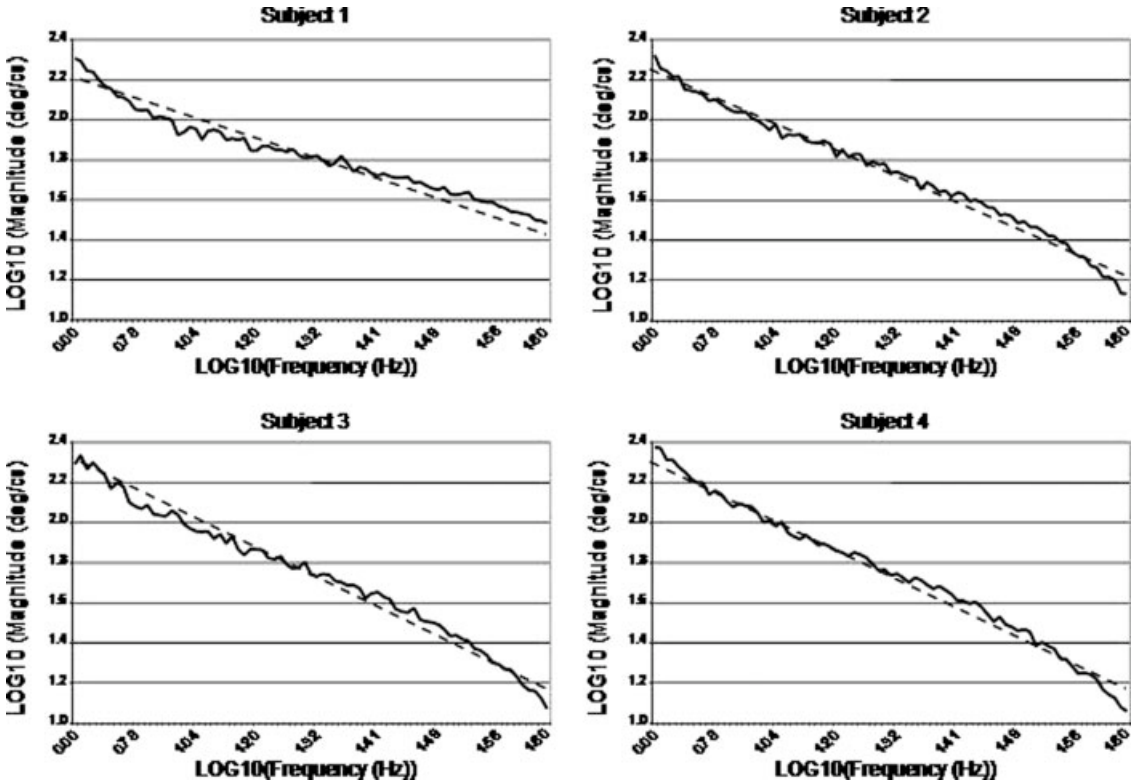

Figure 5.

Examples of the log–log plots of the FFT of the 1st derivatives of EEG phase differences in the anterior-to-posterior direction. Solid line is the FFT spectral values and the dotted line is the linear regression fits to the spectral values. Table II shows the slope or α exponents in the $1/f^{\alpha}$ equation.

duration ("unstable phase dynamics") and the phase locking interval ("stability"), however, the correlations were relatively small indicating that the majority of variance is unaccounted for when correlating phase shift durations with phase locking intervals.

To further explore the nature of phase shift and phase duration the temporal boundaries and frequency distributions were studied. Figure 9 shows the frequency distribution of phase shift durations (Top) and the phase locking intervals (Bottom) for short and long distance connections (average of left and right hemisphere) in 215 subjects between 10 and 16.67 years of age. Phase shift duration exhibited temporal boundaries or "window lengths" with no durations less than 25 msec and no durations greater than 100 msec. Local (6 cm) frontal distances exhibited the most peaked distribution at 45 msec duration and the long distance (24 cm) connections were shifted in peak duration by ~15–20 msec. The phase locking interval exhibited temporal boundaries or window lengths with no durations less than 150 msec and 99% of the durations less than 900 msec. The frequency distributions as a function of distance were similar although the long distance (24 cm) connections were most peaked at 200 msec and exhibited an ~50 msec. shift in peak duration in comparison to the local connections. Phase locking (stable dynamic) was on the average shorter and phase shift duration (unstable dynamic) was longer in the long distant connection system.

Developmental Oscillations

Examination of Figures 7 and 8 shows ultra-slow oscillations with inter-peak intervals of ~2–3 years. Spectral analyses of the developmental time series of mean phase shift duration from 0.4–16.2 years for the 6 and 24 cm inter-electrode distances are shown in Figure 10. The top row is the frontal-to-posterior electrode combinations and the bottom

TABLE II. Linear regression fit to the log–log plot of the power spectrum of EEG phase reset

Regressions	Subject 1	Subject 2	Subject 3	Subject 4
Slope – α	0.5419	0.7543	0.8066	0.8634
Correlation	0.966	0.917	0.914	0.918
Significant	$P < 0.0001$	$P < 0.0001$	$P < 0.0001$	$P < 0.0001$

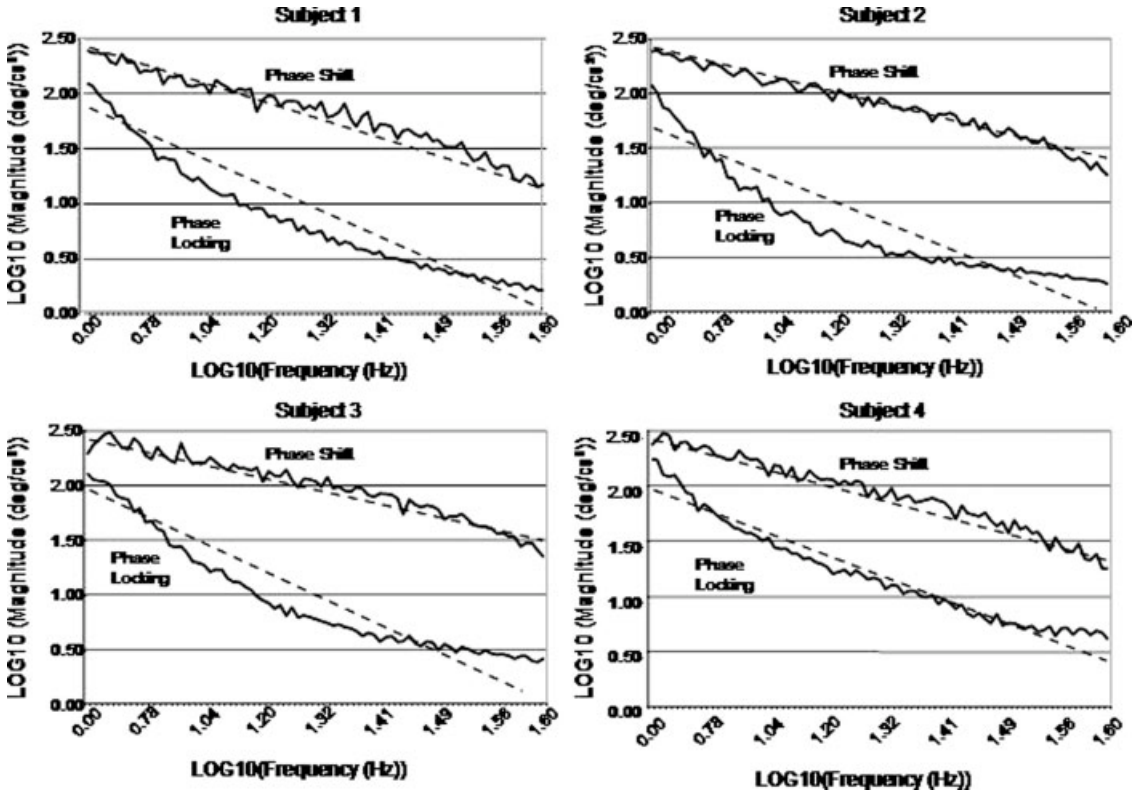

Figure 6.

Log–log plots of the Fourier analyses of the 1st derivative of phase differences during periods of phase locking versus periods of phase shift in the four different subjects in Figure 5. Solid line is the FFT spectral values and the dotted line is the linear regression fits to the spectral values. A $1/f^{\alpha}$ distribution is present in all instances in which the slope coefficients were higher for the phase locking periods in comparison to the phase shift periods. Table III shows the differences in slopes and the $1/f$ α coefficients for phase shifting versus phase locking as well as the average $\alpha \approx 1$.

row is the occipital-to-anterior combinations. The left column is the left hemisphere mean FFT values and the right column is the right hemisphere values (see Fig. 1). In general, there was greater developmental spectral energy in the short inter-electrode distance (6 cm) in comparison to the long inter-electrode distance (24 cm). Most of the developmental spectral energy was in the ultraslow frequency range of 1 cycle per lifespan (i.e., a wavelength of 16 years) to ~12 cycles per lifespan (i.e., a wavelength of 1.3 years). The highest peak frequency was 31 cycles per lifespan (i.e., a wavelength of 0.5 years or 6 months).

Spectral analyses of the developmental time series of mean phase locking intervals from 0.4–16.2 years for the 6 and 24 cm inter-electrode distances are shown in Figure 11 The top row of figure 11are the anterior-to-posterior electrode combinations and the bottom row are the posterior-to-anterior combinations. The left column is the left hemisphere FFT values and the right column is the right hemisphere values (see Fig. 1). Similar to phase shift duration, phase locking exhibited most of the spectral energy in the ultraslow frequency range of 1 cycle per lifespan (i.e., a wavelength of 16 years) to ~20 cycles per lifespan (i.e., a wavelength of 0.8 years). Similar to phase shift duration, phase locking in the short inter-electrode distance (6 cm) was greater than the long distance (24 cm) in the posterior-to-anterior direction.

Tables VII and VIII are summaries of the cycles per lifespan (cpl) and the wavelength (16 yrs/cpl) of the spectral peaks in the FFT analyses of the mean duration of phase shift and mean phase locking developmental trajectories from 0.4–16.2 years shown in Figures 9 and 10, respectively. Table VII shows the FFT peak values for phase shift duration over the lifespan in the frontal-to-posterior direction (Top) and for the posterior-to-anterior direction

TABLE III. Linear regression fit of separate log–log spectral analysis of phase shift and phase locking

Regressions	Subject 1	Subject 2	Subject 3	Subject 4
Phase lock – α	1.4223	1.3207	1.3764	1.2088
Phase shift – α	0.8226	0.7453	0.6826	0.7938
Average – α	1.1225	1.0330	1.0295	1.0013
T-test	$P < 0.0001$	$P < 0.0001$	$P < 0.0001$	$P < 0.0001$

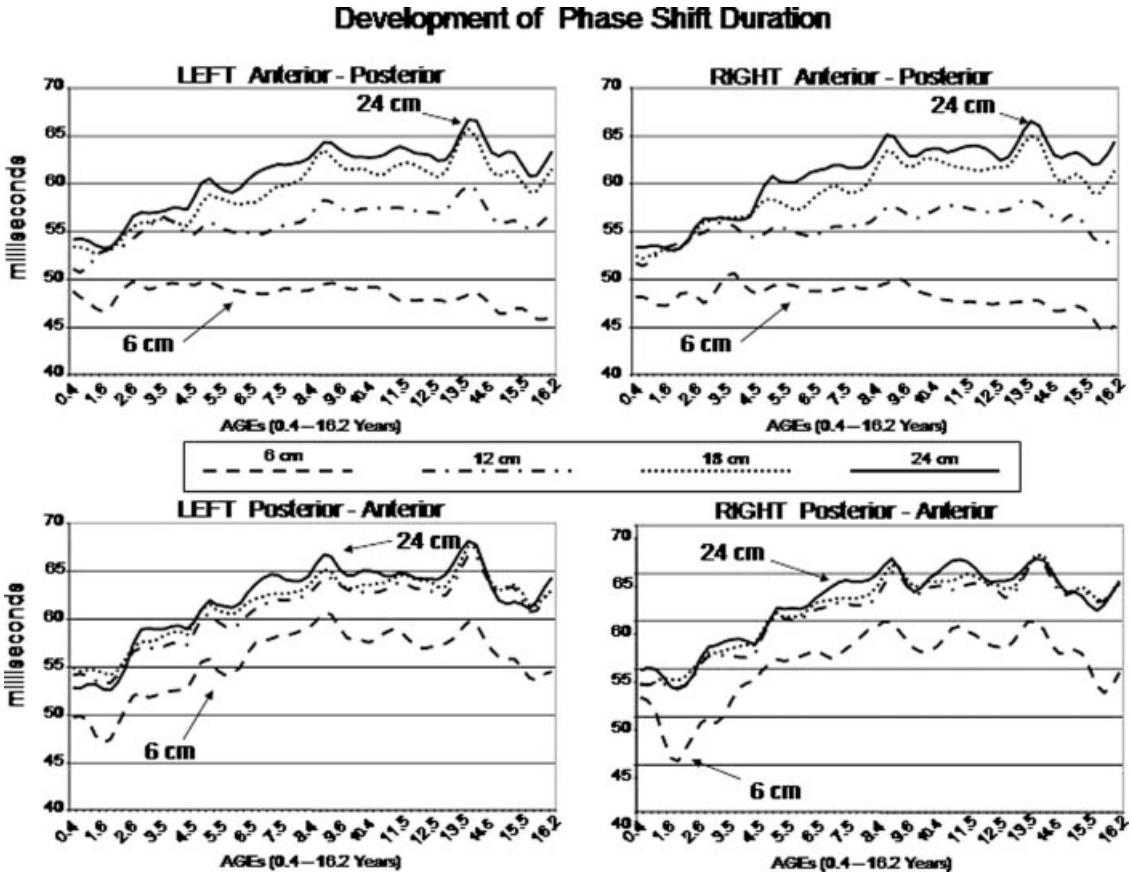

Figure 7.

Mean EEG phase shift duration from 0.4 to 16.2 years of age. Top row are from the anterior-to-posterior electrode combinations and bottom row are from the posterior-to-anterior electrode combinations (see Fig. 1). The left column is from the left hemisphere and the right column is from the right hemisphere. It can be seen that phase shift duration increases in most electrode combinations but decreases in the short inter-electrode distance (6 cm) in the anterior-to-posterior direction.

(Bottom). It can be seen that short (6 cm) and distant (24 cm) exhibited different spectra for phase shift duration and different spectra as a function of direction. In general, there are more spectral peaks and greater power in the long distant inter-electrode connections (24 cm) in the anterior-to-posterior direction while there are more spectral peaks in the 6 cm distance in the posterior-to-anterior direction.

Table VIII are summaries of the cycles per lifespan (cpl) and the wavelength (16 yrs/cpl) for the mean phase locking developmental trajectories from 0.4–16.2 years. The largest number of spectral peaks was in the posterior-to-anterior direction in the short inter-electrode distance (6 cm).

DISCUSSION

This study extends the investigation of the spatial and temporal properties of EEG PR to a large population of subjects from infancy to adolescence and focuses on brain development of PR in the alpha frequency band. An important finding is that the average phase shift duration (unstable dynamics) and the average phase locking interval (stability) were significantly correlated with age and exhibited different maturational trajectories, oscillations and growth spurts in the anterior-to-posterior versus posterior-to-anterior directions (see Figs. 7 and 8). A second significant finding was that the frontal phase shift duration (unstable dynamics) increased as a function of age in distant connections in contrast to posterior local connections (see Fig. 7 and Table IV). The third significant finding was that phase stability increased as a function of age in both local and distant connections (see Fig. 8 and Table V). A fourth significant finding was the presence of $1/f^{\alpha}$ log–log distributions near to 1 thus showing scale invariant fluctuations linked to the development of minimally stable states such as human EEG PR (see Figs. 5 and 6 and Tables II & III). All five null hypotheses listed in the introduction were rejected by the findings in this study.

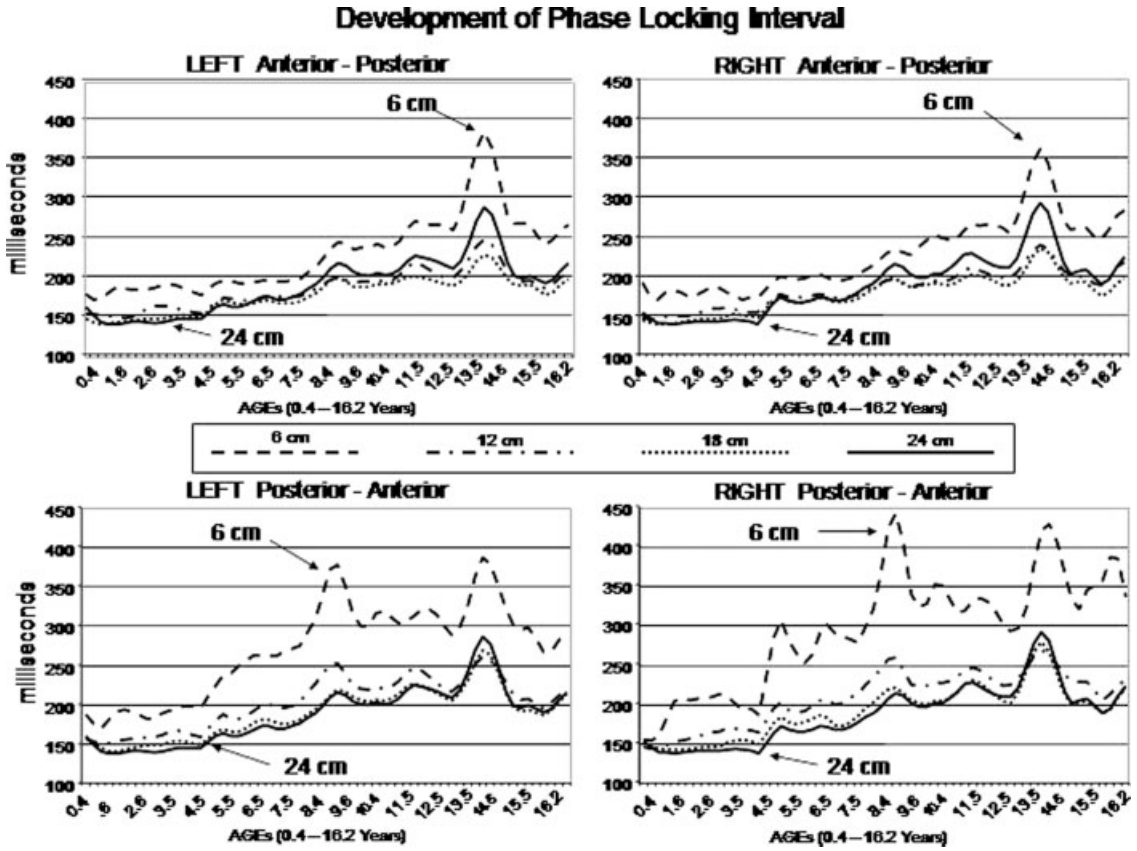

Figure 8.

Mean EEG phase locking intervals from 0.4 to 16.2 years of age. Top row are from the anterior-to-posterior electrode combinations and bottom row are from the posterior-to-anterior electrode combinations (see Fig. 1). The left column is from the left hemisphere and the right column is from the right hemisphere. Growth spurts and oscillations during development are seen. Also, it can be seen that phase locking intervals increase as a function of age in all electrode combinations.

TABLE IV. Age regression of phase shift duration

	6 cm	12 cm	18 cm	24 cm
Left anterior – posterior				
Slope (msec/0.25 year)	−0.1	0.3	0.6	0.6
Intercept (msec)	49.4	53.6	54.4	55.4
Correlation	−0.534	0.700	0.833	0.844
Significant	$P < 0.0001$	$P < 0.0001$	$P < 0.0001$	$P < 0.0001$
Right anterior – posterior				
Slope (msec/0.25 year)	−0.2	0.2	0.6	0.7
Intercept (msec)	49.4	53.8	54.3	54.8
Correlation	−0.577	0.633	0.823	0.861
Significant	$P < 0.0001$	$P < 0.0001$	$P < 0.0001$	$P < 0.0001$
Left posterior – anterior				
Slope (msec/0.25 year)	0.5	0.6	0.6	0.6
Intercept (msec)	51.6	56.5	56.4	55.4
Correlation	0.634	0.731	0.819	0.844
Significant	$P < 0.0001$	$P < 0.0001$	$P < 0.0001$	$P < 0.0001$
Right posterior – anterior				
Slope (msec/0.25 year)	0.5	0.7	0.7	0.7
Intercept (msec)	51.1	56.3	55.5	54.8
Correlation	0.628	0.771	0.841	0.861
Significant	$P < 0.0001$	$P < 0.0001$	$P < 0.0001$	$P < 0.0001$

TABLE V. Age regression of phase locking interval

	6 cm	12 cm	18 cm	24 cm
Left anterior – posterior				
Slope (msec/0.25 year)	8.7	4.5	4.3	6.5
Intercept (msec)	155.0	145.7	139.2	132.4
Correlation	0.825	0.852	0.868	0.831
Significant	$P < 0.0001$	$P < 0.0001$	$P < 0.0001$	$P < 0.0001$
Right anterior – posterior				
Slope (msec/0.25 year)	8.7	4.7	4.4	0.0068
Intercept (msec)	153.8	144.0	139.5	130.8
Correlation	0.870	0.905	0.859	0.840
Significant	$P < 0.0001$	$P < 0.0001$	$P < 0.0001$	$P < 0.0001$
Left posterior – anterior				
Slope (msec/0.25 year)	10.1	5.5	5.6	6.5
Intercept (msec)	187.1	156.8	141.9	132.4
Correlation	0.783	0.781	0.819	0.831
Significant	$P < 0.0001$	$P < 0.0001$	$P < 0.0001$	$P < 0.0001$
Right posterior – anterior				
Slope (msec/0.25 year)	13.1	6.3	5.9	6.8
Intercept (msec)	186.7	156.6	142.3	130.8
Correlation	0.824	0.833	0.821	0.840
Significant	$P < 0.0001$	$P < 0.0001$	$P < 0.0001$	$P < 0.0001$

EEG Phase Transitions and Self-Organized Criticality

The results are consistent with self-organized criticality (SOC) models of cortical function [Bak et al., 1988; Buzsaki, 2006; Freeman et al., 2003, 2006; Le van Quyen, 2003; Linkenkaer-Hansen et al., 2001; Stam and de Bruin, 2004]. Self-organized criticality was defined by Bak et al. [1987, 1988] as the combination of "self-organization" and "criticality" necessary to describe complex systems in which phase transitions spontaneously occur without external "tuning" or external influences. PR includes "self-organization" in the form of phase locking and "criticality" in the form of rapid phase shifts. There are no known sources of the phase shift transitions themselves and thus, phase shifts are likely a widely distributed "emergent" process that spontaneously occurs in complex systems. A fundamental property of SOC is the presence of $1/f^{\alpha}$ distributions that characterize invariant scaling properties, fractal spatial statistics and long-range spatial and temporal correlations, where f = frequency and $\alpha \approx 1$ [Bak et al., 1987, 1988; Nikulin and Brismar, 2004, 2005; Parish et al., 2004]. Studies by Rios and Zang [1999] have shown that the universal properties of the $1/f^{\alpha}$ distribution are an activation-deactivation sequence of a "slow" energy addition and a "fast" energy dissipation with the additional condition of a preferred propagation direction and a limited range of energy dissipation. According to Bak et al. [1987, 1988], Bak [1996] and Rios and Zang [1999] if these universality properties exist, then a $1/f$ distribution will be produced. EEG PR meets the slow and fast component criteria with rapid phase shift onsets as a "fast process" (5–20 msec) and phase locking as a comparative "slow process" [150 msec to 1 sec; Freeman et al., 2006]. All self-sustained oscillators, such as neurons, are characterized by the fact that they dissipate energy [Pikovsky et al., 2003], thus the SOC energy dissipation criterion is also met when measuring EEG PR. The exact physiological mechanisms of the conditional criteria of limited energy dissipation and preferred direction are likely related to the number and strength of connections and synaptic drives within and between clusters of neurons although detailed experimentation to test or quantify the physiological mechanisms have not as yet been conducted to the best of our knowledge.

Feigenbaum [1983] evaluated nonlinear systems in "criticality transitions" during the period of transition from quasi-periodic behavior to "chaos" and discovered that the expansion around this point is a $1/f^{\alpha}$ distribution. In other words the complex state at the border between predictable oscillatory behavior and unpredictable chaos is the "Pink Noise" distribution called "one-over-f ". As pointed out by Bak [1996], Freeman et al. [2003, 2006] and Buzsaki [2006] the brain approaches "chaos" followed by a transition to periods of phase locking. Understanding the details of the Feigenbaum's "Critical Point" during the transition from predictable behavior to "Chaos" is referred to as the Universality principle that was expanded by Haken [1983] to a general mathematical solution using a small set of "order parameters" to control the behavior of higher ordered systems. Once the value of the exponent in the $1/f^{\alpha}$ equation

TABLE VI. Correlations between coherence and phase shift duration and phase locking interval

	Phase shift	Phase locking
Coherence	−0.547	0.863
Phase shift	—	−0.386
Phase locking	−0.386	—

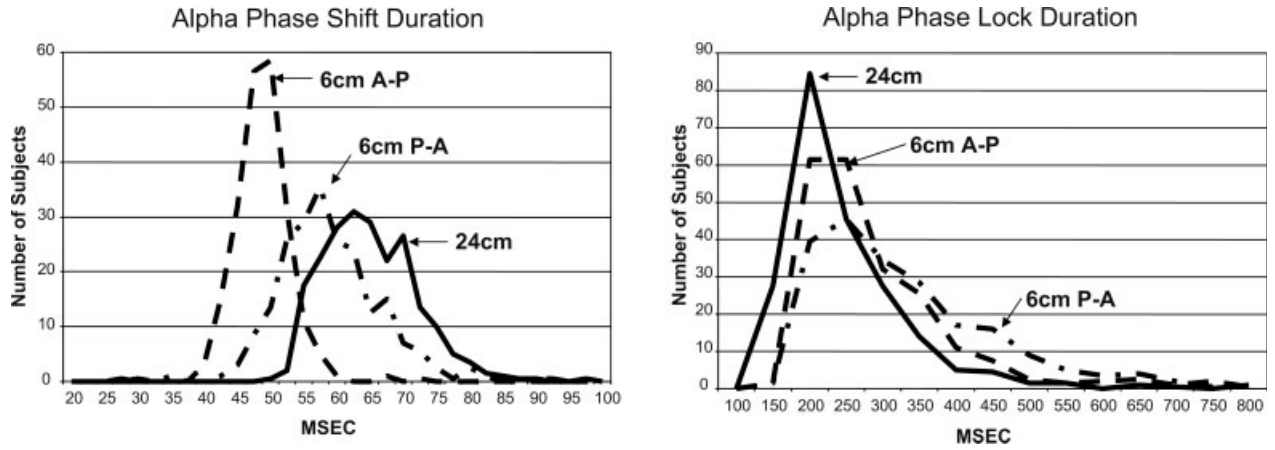

Figure 9.

Frequency histograms of phase shift duration (Top) and phase lock duration (Bottom) from 215 subjects between 10 and 16.67 years of age. 6 cm anterior-to-posterior (AP) interelectrode distance, 6 cm interelectrode distance for posterior-to-anterior direction (PA) and the long (24 cm) inter electrode distance which is the same for AP and PA (see fig. 1). Left and right hemispheres were averaged together. The y-axis is the number of subjects and the x-axis is msec.

is known then the mathematics of SOC are more tractable [Pikovsky et al., 2003; Rios and Zang, 1999]. Future analyses of the 1st and 2nd derivatives of phase shift onset and offset may provide information about the energies involved in the transition from stability to "unstable phase dynamics" or when the brain briefly approaches "chaos."

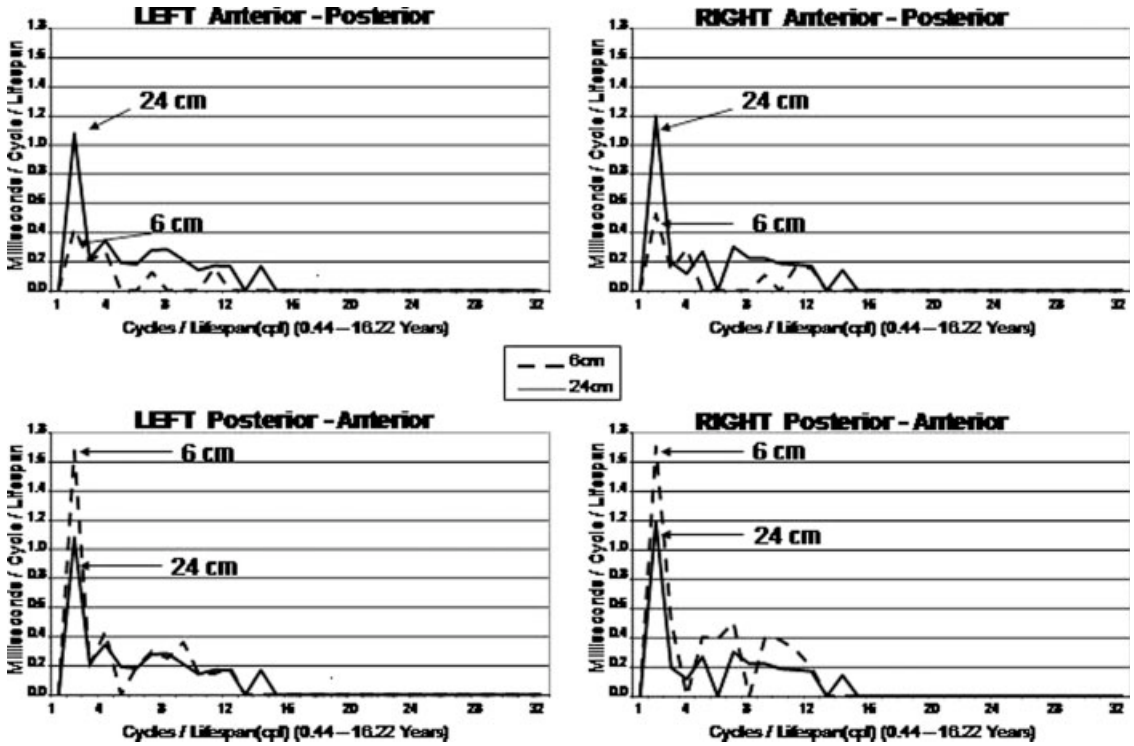

Figure 10.

Fourier spectral analyses of the developmental trajectories of phase shift duration from 0.4 years to 16.2 years of age in short (6 cm) (dashed line) and long (24 cm) (short line) inter-electrode distances in the anterior-to-posterior and posterior-to-anterior directions. Magnitude is on the *y*-axis and frequency on the *x*-axis. Distant inter-electrodes exhibited greater power in the anterior-to-posterior direction while local connections exhibited the greater power in the posterior-to-anterior direction.

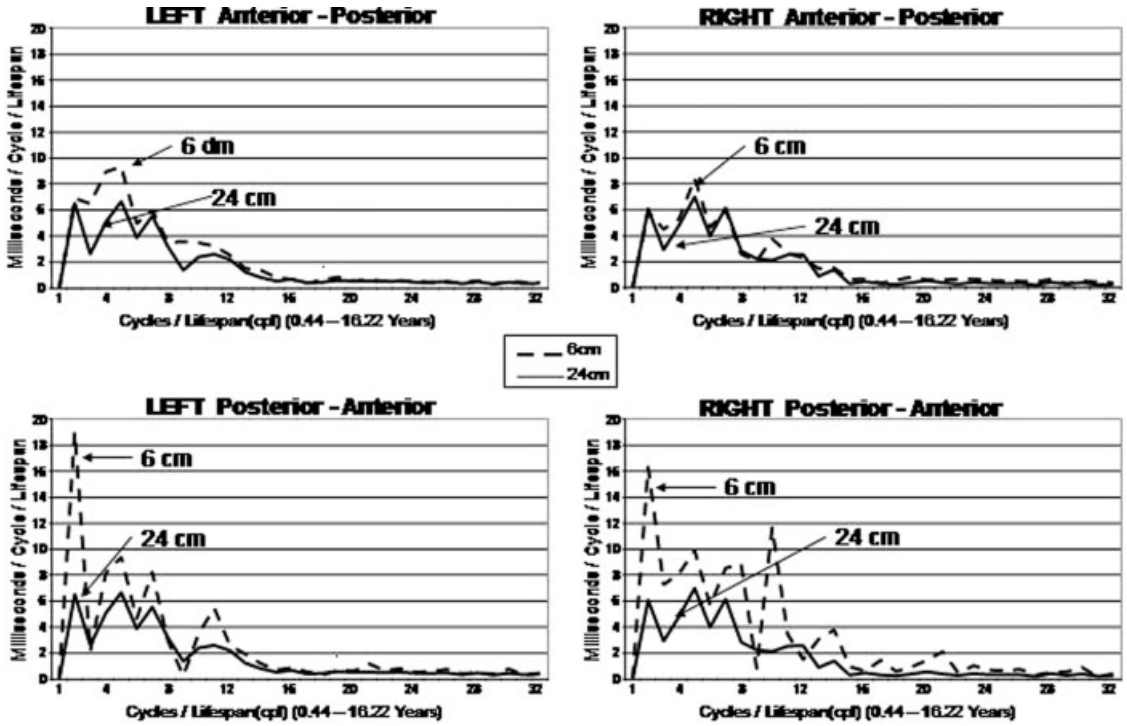

Figure 11.

Fourier spectral analyses of the developmental trajectories of mean phase locking from 0.4 years to 16.2 years of age in short (6 cm) (dashed line) and long (24 cm) (solid line) inter-electrode distances in the anterior-to-posterior and posterior-to-anterior directions. Magnitude is on the *y*-axis and frequency on the *x*-axis. The greatest spectral energy was in the short distance inter-electrodes (6 cm) in the posterior-to-anterior direction.

Long-Range Temporal and Spatial Correlations

As emphasized by Buzsaki [2006] and Freeman et al. [2003, 2006] an attractive feature of SOC is its ability to describe complex systems behavior by simple power laws. The presence of the $1/f^{\alpha}$ distribution is a tell tale sign of self-organization and also measures the length of the correlation or "spatial and temporal memory effects" in the EEG signal. The slope of the log–log fit to the spectral distribution is an estimate of the temporal-range of the correlation in which the closer the slope approximates 1.0 then the stronger the long-range temporal correlations [Nikulin and Brismar, 2005; Stam and de Bruin, 2004]. A possible spatial correlation is the differential rates of change in PR in the frontal lobes versus the posterior cortical regions. For example, over the lifespan phase shift duration was flat in the short distance compartment but grew significantly (~12 msec) in the long distance compartment (see Fig. 7). The upward growth slope and the rapid growth spurts are nonlinear and can be fit by exponentials. This is important because in SOC models dynamic scaling is observed at equilibrium critical points where the power-law correlations in time are generated by long-range correlations in space [Bak et al., 1987, 1988].

In the present study, we showed that the two components of PR (i.e., phase locking interval and phase shift duration) exhibit different coefficients in the $1/f^{\alpha}$ function where phase locking spectra exhibited a shorter temporal memory effect then the "unstable phase dynamics" which exhibited a longer-range scaling effect (see Fig. 6 and Table III). The scale invariant properties of $1/f$ reflect the temporal scaling of events that pre-date the occurrence of critical events and in the case of EEG phase locking there is reduced influence by past events and there is shorter spatial scaling. In contrast, phase shift duration is when phase stability is minimal and the brain approaches "chaos" with a period of high uncertainty and long-range temporal memory.

Another unique finding in this study is the observation of age dependent and ultra-slow changes in PR from infancy to adolescence (Figs. 9 and 10). Growth spurts at age 9 and age 14 coincide with important behavioral developmental stages as hypothesized by Piaget [1975] and other developmental theorists [Case, 1985, 1987; Fischer, 1987; Fischer et al., 2007]. These developmental theorists share a general theoretical assumption of the maturation of neural connections by genetic factors that are oscillatory with regular intervals. The findings in this study are

TABLE VII. Summary of developmental spectral peaks of phase shift duration

Phase shift duration			
6 cm		24 cm	
CPL	λ (years)	CPL	λ (years)
Anterior – posterior			
Left			
2	8	2	8
4	4	4	4
7	2.29	7	2.29
11	1.45	8	2
		12	1.33
		14	1.14
Right			
2	8	2	8
4	4	5	3.2
9	1.78	7	2.29
11	1.45	12	1.33
		14	1.14
Posterior – anterior			
Left			
2	8	2	8
4	4	4	4
7	2.29	7	2.29
9	1.78	14	1.14
12	1.33		
Right			
2	8	2	8
5	3.2	5	3.2
7	2.29	7	2.29
9	1.78	14	1.14
10	1.6		

consistent with these developmental models as well as identical and non-identical twin studies of the development of EEG coherence [van Baal et al., 2001; Van Beijsterveldt et al., 1998]. The rhythmic order and cycles of PR are likely due to fundamental molecular processes involved in the production and elimination of synapses [Kandel, 2007; Thatcher, 1992, 1994; Thatcher et al., 1987, 1998]. This is likely the case because EEG amplitude varies primarily as a function of the number, strength and phase locking of synaptic potentials [Niedermeyer and Lopes da Silva, 2005; Nunez, 1981, 1995]. In the present study, environmental influences that affect the strength of cortical synaptic potentials are averaged over diversely different family experiences and different urban and rural environments. This fact tends to narrow the search for a causal link between slow rhythmic change in PR to slow rhythmic changes in the number of synaptic connections and less to short term rhythmic changes in the environmentally driven strength of synaptic connections.

Temporal Boundaries of EEG Phase Reset

Shallace [1964], Allport [1968], Efron [1967, 1970a,b], and others Sanford [1971], Varela [1995] have shown a minimum perceptual frame from ~40 msec for auditory stimuli to 140 msec for visual stimuli required to temporally distinguish events as being successive in time. These studies as well as others show that learning-dependent changes in neural networks is not a continuous process but rather a discontinuous sequencing of narrow time windows [John, 2005; Thatcher and John, 1977]. Event related desynchonization (ERD) studies show an ~200 msec delay between the onset of an event and a maximum amplitude reduction which extends until ~650 msec followed by a resynchronization (ERS) of increasing EEG amplitude about 900–2000 msec [Klimesch et al., 2007]. The findings in this study may have relevance to perceptual frames and ERD by considering phase shift duration and phase locking intervals as elemental "atoms" or "quanta" that underlie perceptual frames and ERD. For example, Figure 9 (Top) showed that PR is temporally bounded with a minimal phase shift duration of about 40 msec and a maximum phase shift duration of about 90 msec. Phase shift is followed by phase locking which, as seen in Figure 9 (Bottom), is also bounded from about 150 msec to about 800 msec with the most frequent phase locking intervals between 200 and 350 msec. Phase shift and phase locking are ongoing spontaneous processes that occur over widespread regions of the neocortex in resting conditions such as in the present study as well as during tasks. Whether or not the phase shift and phase locking are time locked to a task is irrelevant since "self-organizing criticality" is an ongoing back-

TABLE VIII. Summary of developmental spectral peaks of phase locking intervals

Phase locking interval			
6 cm		24 cm	
CPL	λ (years)	CPL	λ (years)
Anterior – posterior			
Left			
2	8	2	8
4	4	5	3.2
5	3.2	7	2.29
7	2.29	11	1.45
Right			
2	8	2	8
5	3.2	5	3.2
7	2.29	7	2.29
10	1.6	12	1.33
Posterior – anterior			
Left			
2	8	2	8
5	3.2	5	3.2
7	2.29	7	2.29
11	1.45		
21	0.76		
Right			
2	8	2	8
5	3.2	5	3.2
8	2	7	2.29
10	1.6	12	1.33
14	1.14	14	1.14
21	0.76		

ground emergent process that on the average produces a 40–90 msec period of phase shift "uncertainty" or approximate "chaos" followed on the average by a 200–650 msec period of phase locking or "stability". This background process results in "blank" periods when large assemblies of neurons are in a PR mode (i.e., phase shift and phase locking). A type of "refractory" period is when phase locked neurons are unavailable for allocation by a different cluster of neurons at a different moment of time. Phase locking of a subset of a local cluster of neurons can result in a reduction in the amplitude of the surface EEG because phase locking occurs over long distances and thus reduces the size of the cluster of "idling" neurons by spatial differentiation. The findings in this study are consistent with models of event related desynchronization (ERD) in which the background PR as well as stimulus locked PR contribute to the ERD [Klimesch et al., 2007]. This hypothesis of linking PR during the background spontaneous EEG to ERD provides a new definition of the term "desynchronization" used to describe event related desynchronization (ERD) in that desynchronization is actually "spatially differentiated phase locking" or "micro bonding" as the underlying mechanism that removes available neurons from the "idling" population of neurons resulting in a reduction in the average amplitude of the post-stimulus EEG.

Local versus Distant Connection Systems

The short inter-electrode distance exhibited stronger developmental changes in the mean phase locking interval than the long inter-electrode distance, especially in the posterior-to-anterior direction. The short inter-electrode distance also exhibited larger growth spurts in phase locking intervals than the long inter-electrode distance connections (see Fig 8). In contrast to phase locking, the mean phase shift duration declined in the local frontal connections while it increased in the long inter-electrode distance (see Fig. 7 and Table IV). This showed that local connections exhibited shorter periods of unstable phase dynamics than the distant connections. In general, long distance connections exhibited longer phase shift durations (i.e., more "instability") than local connections (see Fig. 7). The finding that phase locking intervals only modestly increased with age in the long distance systems but strongly increased in the local connections indicates that maturation is dominated more by local phase locking in comparison to the long distances where there is a slower refinement process involved in the development of the long distance system.

Previous studies have used two compartment models of EEG coherence in which the number of connections and the strength of connections influence the magnitude of coherence [Hanlon and Thatcher, 1999; McAlaster, 1992; Nunez, 1981; Thatcher et al., 1986, 1998, 2007; van Baal et al., 2001; Van Beijsterveldt et al., 1998]. According to these models, a positive correlation between coherence and phase locking is expected since coherence is a measure of phase consistency [Bendat and Piersol, 1980; Otnes and Enochson, 1978]. Also, one would expect a negative correlation between phase shift duration and coherence since phase shift duration is related to unpredictability and reduced phase stability. This study supports the two compartment connection models by demonstrating a significant difference between local versus distant connections with a positive correlation between phase locking intervals ("stability") and coherence and a negative correlation to phase shift duration ("unstable phase dynamics"), especially in the local or short inter-electrode pairs. The findings in this study are also consistent with EEG coherence studies [McAlaster, 1992; Thatcher et al., 1986, 1998, 2007; van Baal et al., 2001; Van Beijsterveldt et al., 1998] which hypothesize that fluctuations of EEG coherence during development are due largely to fluctuations in the number of cortical synaptic connections.

A simple and unifying mathematical model that links the development of the number and/or density of synaptic connections to EEG coherence [Thatcher, 1994; Thatcher et al., 2007] and to the two components of PR, i.e., "Unstability" (phase shift duration) and "Stability" (phase lock duration) is shown in equation 11:

$$N_{ij} \Longrightarrow K \frac{S_{ij}}{C_{ij}} \tag{11}$$

where N_{ij} = the number and/or density of local synaptic connections in a matrix, K_{ij} = a proportionality constant, S_{ij} = "Stability" defined as the average phase lock duration and C_{ij} = "Unstable phase dynamics" defined as the average phase shift duration. S_{ij}/C_{ij} is the chaos to stability ratio where the number and/or density of synaptic connections is inversely related to the tendency toward "chaos" and directly related to stability. During short periods of time the relationship on each side of the equals sign is likely a two-way relationship, however, the arrow symbol $\Rightarrow$ represents the slow developmental trend over a lifespan which gives greater weight to the relationship between the number of synaptic connections as influencing "unstability" and "stability" rather than the reverse direction. Certainly, phase locking or phase synchrony is important for learning, perception and memory and thus the environment must be an important factor in determining the number of connections between different brain regions as well as the dynamics of PR. However, the oscillations and growth spurts in PR are averages over the lifespan from environmentally diverse subjects and thus, there is greater weight given to the number and/or density of synaptic connections as determining the balance between "unstable phase dynamics" and "stability" over the maturation period from infancy to adolescence. That is, as the number of synaptic connections increases during maturation then phase stability increases and the duration of phase shift "uncertainty" decreases. It is relevant that ecological models of cooperation, competition, independence and predator/prey involving nonlinear regulation of syn-

aptogenesis have been applied to measures of human cortical development [Edelman, 1987; Thatcher, 1994, 1998]. The findings generally support SOC epigenetic models of human brain development where growth spurts are punctuations or "unstable phase dynamics" within periods of stability and the underlying $1/f$ dynamics represent long-range temporal and spatial correlations. The linkage of the number and/or density of synaptic connections to SOC suggest that packing density and the number of synaptic connections may be critical order parameters that determine some of the dynamics of cortico-cortical coupling during human development.

Differences in the Anterior-to-Posterior Versus the Posterior-to-Anterior Direction

The strongest difference between the anterior-to-posterior versus the posterior-to-anterior direction of electrode placement are the phase shift duration differences in the short inter-electrode distances. The development of EEG phase shift duration in the anterior-to-posterior direction exhibited a negative slope with age, whereas the short distances exhibited a positive slope with age in the posterior-to-anterior direction. The development of the magnitude of phase locking intervals was also different in the short inter-electrode distance in the anterior-to-posterior versus the posterior-to-anterior directions. The directional difference in development of phase shift duration and phase locking intervals can be explained by a simple and unifying concept, similar to that to explain EEG coherence and EEG phase differences in local and distant connections [Thatcher et al., 1986, 1998]. The unifying concept is that the findings are consistent with a differential preference for packing density in local brain regions with greater packing density in occipital brain regions in comparison to the frontal lobes. For example, the occipital brain regions have the highest neural packing density and the frontal lobes have the lowest packing density [Blinkov and Glezer, 1968; Carpenter and Sutin, 1983]. The number of connections is related to the packing density by virtue of the available area on dendrites for synaptogenesis [Purves, 1988]. Although high packing density can result in shorter dendrites, nonetheless, with more neurons there are more synaptic connections. This conclusion is consistent with equation 11, where reduced connections are related to increased periods of "unstable phase dynamics" and increased number of connections is related to longer synchronization intervals and shorter periods of unstable dynamics.

As seen in Figures 7 and 9, the mean and mode of phase shift duration is shorter in the frontal lobes than in posterior regions at the same interelectrode distance (i.e., 6 cm). Previous studies have shown that the shorter the phase difference between local frontal regions then the higher is the I.Q. [Thatcher et al., 2005]. The interpretation offered for shorter phase delays and higher I.Q. is that the faster that the frontal lobes orchestrate the resources of the posterior neocortex then the higher the I.Q. [Thatcher et al., 2005]. Because the same subjects are used in the present study as in the earlier Thatcher et al. [2005] study the present findings are consistent with this interpretation and extend the earlier findings to implicate more rapid phase shift as a component of shorter phase delays.

Another finding of interest was that the local or short inter-electrode distances exhibited larger growth spurts (age 9 and age 14) in the posterior-to-anterior direction than in the anterior-to-posterior direction. The occipital-parietal growth spurts at age 9 and 14 may correspond to the development of visual-spatial information processing as well as more abstract aspects of language and cognitive development which occur during these ages [Case, 1985, 1987; Fischer, 1987]. The fact that the largest growth spurts occurred in the phase locking interval and not in phase shift duration suggests that the developmental changes during these age periods involve increased network stability and increased integration in contrast to an increased tendency to "chaos."

Nonlinear Oscillations in SOC and Growth Spurts

The frequency spectrum of the development of phase shift duration and phase locking intervals showed significant ultraslow oscillations over the lifespan from infancy to adolescence. The mean frequency of oscillations were different in the anterior-to-posterior and posterior-to-anterior directions and for different inter-electrode distances but they were similar for left and right hemispheres (see Figs. 9 and 10 and Tables VII and VIII). The strongest spectral magnitudes in the development of phase shift duration and phase locking were repetitive cycles at wavelengths between 8 and 2 years. The highest frequency of oscillations was ~1 year wavelengths and the higher frequency oscillations exhibited the lowest power. Additional studies, such as identical and nonidentical twin studies, can test the genetic contributions to the development of EEG PR. We have found that PR per second while correlated as expected is often unrevealing and masks some of the underlying dynamics because of the short time frame of phase shift duration and the long time frame of phase locking. It is necessary to measure both phase shift duration and the phase locking interval in order to understand PRs per second. Mathematical neural network models of the development of EEG PR can test developmental hypotheses and animal studies can be used to further evaluate the genetics and molecular biology of EEG PR.

ACKNOWLEDGMENTS

We are indebted to Drs. Rebecca McAlaster, David Cantor and Michael Lester and Ms. Sheila Ignasius and Ms. Diane Pruit for their involvement in the recruitment, EEG testing and evaluation of subjects and Rebecca Walker and

Richard Curtin for database management. Informed consent was obtained from all subjects.

REFERENCES

Allport DA (1968): Phenomenal simultaneity and perceptual moment hypotheses. Br J Psychol 59:395–406.

Bak P (1996): How Nature Works: The Science of Self-Organized Criticality. New York: Springer-Verlag.

Bak P, Tang C, Wisenfeld K (1987): Self-organized criticality: An explanation of $1/f$ noise. Phys Rev Lett 59:381–384.

Bak P, Tang C, Wisenfeld K (1988): Self-organized criticality. Phys Rev A 38:364–374.

Beggs JM, Plenz D (2003): Neuronal avalanches in neocortical circuits. J Neurosci 23:11167–11177.

Bendat JS, Piersol AG (1980): Engineering Applications of Correlation and Spectral Analysis. New York: Wiley.

Blinkov SM, Glezer I (1968): The Human Brain in Figures and Tables: A Quantitative Handbook, Basic Books, Inc. New York: Publisher Plenum Press.

Bloomfield P (2000): Fourier Analysis of Time Series: An Introduction. New York: Wiley.

Breakspear M, Terry JR (2002a): Detection and description of nonlinear interdependence in normal multichannel human EEG data. Clin Neurophysiol 113:735–753.

Breakspear M, Terry JR (2002b): Nonlinear interdependence in neural systems: Motivation, theory and relevance. Int J Neurosci 112:1263–1284.

Breakspear M, Williams LM (2004): A novel method for the topographic analysis of neural activity reveals formation and dissolution of 'dynamic cell assemblies'. J Comput Neurosci 16:49–68.

Bruns A (2004): Fourier, Hilbert and wavelet-based signal analysis: Are they really different approaches? J Neurosci Methods 137: 321–332.

Buzsaki G (2006): Rhythms of the Brain. New York: Oxford University Press.

Carpenter MB, Sutin J (1983): Human Neuroanatomy, 8th ed. Baltimore, Maryland: Williams and Wilkins.

Case R (1985): Intellectual Development: Birth to Adulthood. New York: Academic Press.

Case R (1987): The structure and process of intellectual development. Int J Psychol 22:571–607.

Chavez M, Le Van Quyen M, Navarro V, Baulac M, Martinerie J (2003): Spatio-temporal dynamics prior to neocortical seizures: Amplitude versus phase couplings. IEEE Trans Biomed Eng 50:571–583.

Chialvo DR, Bak P (1999): Learning from mistakes. Neuroscience 90:1137–1148.

Cooper R, Winter AL, Crow HJ, Walter WG (1965): Comparison of subcortical, cortical and scalp activity using chronically indwelling electrodes in man. Electroencpehalogr Clin Neurophysiol 18:217–222.

Cosmelli D, David O, Lachaux JP, Martinerie J, Garnero L, Renault B, Varela F (2004): Waves of consciousness: Ongoing cortical patterns during binocular rivalry. Neuroimage 23:128–140.

Damasio AR (1989): Time-locked multiregional retroactivation: A systems-level proposal for the neural substrates of recall and recognition. Cognition 33:25–62.

Davidson J, Schuster HG (2000): $1/f^{\alpha}$ noise from self-organized critical models with uniform driving. Phys Rev E 62:6111–6115.

Edelman GM (1987): Neural Darwinism: The Theory of Neuronal Group Selection. New York: Basic.

Efron E (1967): The duration of the present. Ann NYAcad Sci 138:713–729.

Efron E. (1970a): The relationship between the duration of a stimulus and the duration of a perception. Neuropsychologia 8:37–55.

Efron E. (1970b): The minimum duration of a perception. Neuropsychologia 8:57–63.

Essl M, Rappelsberger P (1998): EEG coherence and refernce signals: Experimental results and mathematical explanations. Med Biol Eng Comput 36:399–406.

Feigenbaum MJ (1983): Universal behavior in nonlinear systems. Phys D 7:16–19.

Fischer KW (1987): Relations between brain and cognitive development. Child Dev 57:623–632.

Fischer KW, Rose TL, Rose SP (2007): Growth cycles of mind and brain: Analyzing developmental pathways of learning disorders. In Fischer KW, Holmes-Bernstein J,Immordino-Yang MH, editors. Mind, Brain and Education in Reading Disorders. MA: Cambridge University Press 101–132.

Freeman WJ (2003): Evidence from human scalp electroencephalograms of global chaotic itinerancy. Chaos 13:1067–1077.

Freeman WJ, Baird B (1987): Relation of olfactory EEG to behavior: Spatial analysis. Behav Neurosci 101:393–408.

Freeman WJ, Rogers LJ (2002): Fine temporal resolution of analytic phase reveals episodic synchronization by state transitions in gamma EEGs. J Neurophysiol 87:937–945.

Freeman WJ, Burke BC, Homes MD (2003): Aperiodic phase re-setting in scalp EEG of β-γ oscillations by state transitions at α-θ rates. Hum Brain Mapp 19:248–272.

Freeman WJ, Homes MD, West GA, Vanhatlo S (2006): Fine spatiotemporal structure of phase in human intracranial EEG. Clin Neurophysiol 117:1228–1243.

Granger CWJ, Hatanka M (1964): Spectral Analysis of Economic Time Series. New Jersey: Princeton University Press.

Gray CM, Konig P, Engel AK, Singer W (1989): Oscillatory responses in cat visual cortex exhibit inter-columnar synchronization which reflects global stimulus properties. Nature (London), 338:334–337.

Hanlon HW, Thatcher RW, Cline MJ (1999): Gender differences in the development of EEG coherence in normal children. Dev Neuropsychol 16:479–506.

Haken H (1983): Synergetics, An Introduction. Berlin: Springer-Verlag.

Jensen O, Lisman JE (1998): An oscillatory short-term memory buffer model can account for data on the Sternberg task. J Neurosci 18:10688–10699.

John ER (1968): Mechanisms of Memory. New York: Academic Press.

John ER (2002): The neurophysics of consciousness. Brain Res Brain Res Rev 39:1–28.

John ER (2005): From synchronous neural discharges to subjective awareness. Prog Brain Res 150:143–171.

Kahana MJ (2006): The cognitive correlates of human brain oscillations. J Neurosci 26:1669–1672.

Kamiński M, Blinowska KJ, Szelenberger W (1997): Topographic analysis of coherence and propagation of EEG activity during sleep wakefulness. Electroencephalogr Clin Neurophysiol 102: 216–227.

Kandel ER (2007): In Search of Memory: The Emergence of a New Science of Mind. New York: Wiley.

Kirschfeld K (2005): The physical basis of α waves in the electroencephalogram and the origin of the "Berger effect." Biol Cybem 92:177–185.

Klimesch W, Sauseng P, Hanslmayr S, Gruber W, Freunberger R (2007). Event-related phase reorganization may explain evoked neural dynamics. Neurosci Biobehav Rev 31:1003–1016.

Lachaux J-P, Rodriguez E, Le Van Quyen M, Lutz A, Martinerie J, Varela FJ (2000): Studying single-trials of phase synchronous activity in the brain. Int J Bifurc Chaos 10:2429–2439.

Le Van Quyen M (2003): Disentangling the dynamic core: A research program for a neurodynamics at the large-scale. Biol Res 36:67–88.

Le Van Quyen M, Foucher J, Lachaux J-P, Rodriguez E, Lutz A, Martinerie J, Varela FJ (2001a): Comparison of Hilbert transform and wavelet methods for the analysis of neuronal locking. J Neurosci Methods 111:83–89.

Le Van Quyen M, Martinerie J, Navarro V, Varela FJ (2001b): Characterizing neurodynamic changes before seizures. J Clin Neurophysiol 18:191–208.

Linkenkaer-Hansen KI, Nikouline VV, Palva JM, Ilmoniemi RJ (2001): Long-range temporal correlations and scaling behavior in human brain oscillations. J Neurosci 21:1370–1377.

Lopes Da Silva FH (1994): Dynamic of electrical activity of the brain, networks, and modulating systems. In: Nunez P, editor. Neocortical Dynamics and Human EEG Rhythms. pp 249–271.

Lopes Da Silva FH, Pijn JP (1995): Handbook of Brain Theory and Neural Networks. Arbib, Cambridge: MIT Press.

McAlaster R (1995): Postnatal cerebral maturation in Down's syndrome children: A developmental EEG coherence study. Int J Neurosci 65:221–2237.

McCartney H, Johnson AD, Weil ZM, Givens B (2004): θ Reset produces optimal conditions for long-term potentiation. Hippocampus 14:684–697.

Netoff TI, Schiff SJ (2002): Decreased neuronal synchronization during experimental seizures. J Neurosci 22:7297–7307.

Niedermeyer E, Lopes da Silva F (2005): Electroencephalograph: Basic Principles, Clinical Applications and Related Fields. Baltimore, Md: Wilkins and Williamson.

Nikulin VV, Brismar T (2004): Long-range temporal correlations in α and β oscillations: Effect of arousal level and test-retest reliability. Clin Neurophysiol 115:1896–1908.

Nikulin VV, Brismar T (2005): Long-range temporal correlations in electroencephalographic oscillations: Relation to topography, frequency band, age and gender. Neuroscience 130:549–558.

Nunez P (1981): Electrical Fields of the Brain. New York: Oxford University Press.

Nunez P (1995): Neocortical Dynamics and Human EEG Rhythms. New York: Oxford University Press.

Oppenheim AV, Schafer RW (1975): Digital Signal Processing. London: Printice-Hall.

Otnes RK, Enochson L (1978): Applied Time Series Analysis. New York: Wiley.

Parish LM, Worrell GA, Cranstun SD, Stead SM, Pennell P, Litt B (2004): Long-range temporal correlations in epileptogenic and non-epileptogenic human hippocampus. Neuroscience 125: 1068–1076.

Piaget J (1975): Biology and Knowledge, 2nd ed. Chicago: University of Chicago Press.

Pikovsky A, Rosenblum M, Kurths J (2003): Synchronization: A Universal Concept in Nonlinear Sciences. New York: Cambridge University Press.

Press WH, Teukolsky SA, Vettering WT, Flannery BP (1994): Numerical Recipes in C Cambridge Univ. press.

Purves D (1988): Body and Brain: A Trophic Theory of Neural Connections. Boston: Harvard University Press.

Rappelsberger P (1989): The reference problem and mapping of coherence: A simulation study. Brain Topogr 2:63–72.

Rios LP, Zang YC (1999): Universal $1/f$ noise from dissipative self-organized criticality models. Phys Rev Lett 82:472–475.

Rizzuto DS, Madsen JR, Bromfield EB, Schultz-Bonhage A, Seelig D, Aschenbrenner-Scheibe R, Kahana MJ (2003): Reset of human neocortical oscillations during a working memory task. Proc Natl Acad Sci USA 100:7931–7936.

Roelfsmema PR, Engel AK, Konig P, Singer W (1997): Visuomotor integraton is associated with zero time-lag synchronization among cortical areas. Nature 385:157–161.

Rudrauf D, Douiri A, Kovach C, Lachaux JP, Cosmelli D, Chavez A, Renault B, Marttinerie J, Le Van Quyen M (2006): Frequency flows and the time-frequency dynamics of multivariate phase synchronization in brain signals. Neuroimage 31:209–227.

Savitzky A, Golay MJE (1964): Smoothing and differentiation of data by simplified least squares procedures. Anal Chem 36: 1627–1639.

Sanford AJ (1971): A periodic basis for perception and action. In: Colquhoun WP, editor. Biological Rhythms and Human Performance. New York: Academic Press.

Shallice T (1964): The detection of change and the perceptual moment hypothesis. Br J Stat Psychol 17:113–135.

Stam CJ, de Bruin EA (2004): Scale-free dynamics of global functional connectivity in the human brain. Hum Brain Map 22:97–109.

Tallon-Baudry C, Bertrand O, Fischer C (2001): Oscillatory locking between human extrastriate areas during visual short-term memory maintenance. J Neurosci 21:RC177.

Tass PA (2007): Phase Resetting in Medicine and Biology. Berlin: Springer-Verlag.

Tass PA, Rosenblum MG, Weule J, Kurths J, Pikovsky A, Volkmann J, aSchnitzler A, Freund HJ (1998): Detection of n:m phase locking from nosy data: Application to magnetoencephalography. Phys Rev Lett 81:3291–3294.

Tesche CD, Karhu J (2000): θ Oscillations index human hippocampal activation during a working memory task. Proc Natl Acad Sci USA 97:919–924.

Thatcher RW (1992): Cyclic cortical reorganization during early childhood. Brain Cognit 20:24–50.

Thatcher RW (1994): Psychopathology of early frontal lobe damage: Dependence on cycles of postnatal development. Dev Pathol 6:565–596.

Thatcher RW (1998): A predator-prey model of human cerebral development. In: Newell K, Molenaar P, editors. Dynamical Systems in Development. New Jersey: L. Erlbaum Assoc 87–128.

Thatcher RW, John ER (1977): Functional Neuroscience, Vol. 1: Foundations of Cognitive Processes. John ER, Thatcher RW, edtiros. Erlbaum Assoc., N.J.

Thatcher RW, Krause P, Hrybyk M (1986): Corticocortical association fibers and EEG coherence: A two compartmental model. Electroencephalogr Clin Neurophysiol 64:123–143.

Thatcher RW, North D, Biver C (2007): Development of cortical connections as measured by EEG coherence and phase delays. Hum Brain Mapp. (In press).

Thatcher RW, Walker RA, Guidice S (1987): Human cerebral hemispheres develop at different rates and ages. Science 236:1110–1113.

Thatcher RW, Walker RA, Biver C, North D, Curtin R (2003): Quantitative EEG Normative databases: Validation and Clinical Correlation, J Neurotherapy, 7 (No. 3/4):87–122.

Thatcher RW, Biver C, McAlaster R, Salazar AM (1998): Biophysical linkage between MRI and EEG coherence in traumatic brain injury. Neuroimage 8:307–326.

Thatcher RW, North D, Biver C (2005): EEG and intelligence: Univariate and multivariate comparisons between EEG coherence, EEG phase delay and power. Clin Neurophysiol 116:2129–2141.

Vaadia E, Haalman L, Abeles M, Bergman H, Prut Y, Slovin H, Aertsen A (1995): Dynamics of neuronal interactions in monkey cortex in relation to behavior events. Nature 373:515–518.

Varela FJ (1995): Resonant cell assemblies: A new approach to cognitive functions and neuronal locking. Biol Res 28:81–95.

Varela FJ, Lachaux J-P, Rodriguez E, Martinerie J (2001): The brainweb: Phase synchronization and large-scale integration. Nat Rev Neurosci 2:229–239.

van Baal GC, Boomsma DI, de Geus EJ (2001): Longitudinal genetic analysis of EEG coherence in young twins. Behav Genet 31:637–651.

Van Beijsterveldt CE, Molenaar PC, de Geus EJ, Boomsma DI (1998): Genetic and environmental influences on EEG coherence. Behav Genet 28:443–453.

Winfree AT (1980): The Geometry of Biological Time. New York: Springer.